

DISS  
EAR  
298

A dissertation presented to the Department  
of Earth Sciences, Quaid-i-Azam University  
Islamabad for the partial fulfilment of the  
requirement for a MASTER DEGREE IN GEOPHYSICS.



QUAID-I-AZAM UNIVERSITY  
DEPARTMENT OF EARTH SCIENCES

No. DES(SR-6)/86-

Dated:

FINAL APPROVAL OF THESIS

This is to certify that we have read the thesis submitted by MR. MUHAMMAD ARSHAD and accept it for the award of M. Sc. degree in Geophysics.

COMMITTEE:

1. EXTERNAL EXAMINER
2. DR. MUBARIK ALI  
Supervisor (Geophysics)  
Assistant Professor.



A handwritten signature in blue ink, appearing to read 'Arshad', is written over a horizontal dashed line.

3. DR. ABDUL RAUF  
Supervisor (Geology)  
Assistant Professor.



A handwritten signature in blue ink, appearing to read 'Abdul Rauf', is written over a horizontal dashed line.

4. DR. KHAWAJA AZAM ALI  
Chairman  
Deptt. of Earth Sciences  
Quaid-i-Azam University  
Islamabad.



A handwritten signature in blue ink, appearing to read 'Khawaja Azam Ali', is written over a horizontal dashed line.

C O N T E N T S

# C O N T E N T S

## ACKNOWLEDGEMENT

## ABSTRACT

CHAPTER-1:	INTRODUCTION TO THE PROJECT	
1.1	Introduction	2
1.2	Previous Work	3
1.3	Formulation of the Project	4
CHAPTER-2:	TECTONIC HISTORY & REGIONAL GEOLOGY	
2.1	Tectonic History	5
2.2	Regional Geology	7
2.3	Structure	9
CHAPTER-3:	GRAVITY PROSPECTING	
3.1	Gravity Prospecting	13
	3.1.1 Introduction	13
3.2	Gravity Surveys	15
	3.2.1 General	15
	3.2.2 Regional Surveys	16
	3.2.3 Reconnaissance Surveys	16
	3.2.4 Detailed Surveys	16
CHAPTER-4:	GRAVITY SURVEY IN THE PROJECT AREA	
4.1	Gravity Survey in the Project Area	18
	4.1.1 General	18
4.2	Function of Worden Gravimeter	18
4.3	Establishment of Base Station	19

4.3.1	General	19
4.3.2	Establishment of Zero Point (ISD) as Main Base.	20
4.3.3	Computation of Absolute Gravity at the Base.	20
4.3.4	Auxiliary Base Stations	21
4.4	Acquisition of Gravity Data	22
4.4.1	Procedure	22
4.4.2	Acquisition of Altimeter Data	23
	4.4.2.1 General	23
	4.4.2.2 Data Collection	23
4.5	Reduction of Altimeter Data	24
4.5.1	General	24
4.5.2	Temperature Correction	24
4.5.3	Barometric Correction	25
4.6	Reduction of Gravity Data	27
4.6.1	General	27
4.6.2	Drift Correction	28
4.6.3	Latitude Correction	29
4.6.4	Elevation Correction	29
4.6.5	Terrain Correction	30
4.7	Calculation of Crustal Thickness	31
4.8	Estimation of Errors	32
4.8.1	Error due to Inaccurate Heights	32
4.8.2	Error due to Inaccurate Horizontal Control	32
4.8.3	Error due to Inaccurate Density	32
4.8.4	Observational Error	33
4.8.5	Error due to Inaccurate Base Connection	33
4.8.6	Overall Accuracy of the Gravity Survey	34

CHAPTER-5:	SEPARATION OF REGIONAL & RESIDUAL	
5.1	Separation of Regional and Residual Anomalies	35
5.1.1	Introduction	35
5.1.2	Trend Surface Analysis	36
5.1.3	Application of Trend Surface Analysis to Present Case	39
CHAPTER-6:	INTERPRETATION	
6.1	General	41
6.2	Qualitative Interpretation	41
6.2.1	Integrated Study of Elevation and Free-air Anomaly Profiles	42
6.2.2	Integrated Study of Free-air Anomaly and Bouguer Anomaly (Without Terrain Correction) Profiles.	44
6.2.3	Integrated Study of Bouguer Anomaly Profiles With and Without Terrain Correction	45
6.2.4	Interpretation of Bouguer Anomaly Profiles in Context of Geological and Tectonic Maps	45
6.2.5	Qualitative Interpretation of Regional Gravity Anomaly Map	47
6.3	Quantitative Interpretation	49
6.3.1	Two-dimensional Modelling	49
6.3.2	Crustal Thickness	50
CHAPTER-7:	RESULTS	
7.1	Discussion	63
7.2	Conclusions	65
REFERENCES		67
APPENDICES		69

## ACKNOWLEDGEMENT

I am extremely grateful to Dr. Mubarik Ali and Dr. Abdul Rauf for their aspiring and stimulating supervision which led to the successful completion of this Thesis. Thanks are due to Dr. Khawaja Azam Ali and Mr. Ishtiaq A. Jadoon for their invaluable comments.

Special thanks are paid to Dr. I.R. Qureshi of New South Wales University, Australia for his generous help and guidance in the initial stages of the project.

My gratitude is also received by Mr. Nazim-ud-Din and Mr. Munawar Tiwana of Computer Centre, Quaid-i-Azam University, for their generosity and cooperation. I am thankful to Mr. Rafi Ullah Khan for typing this Thesis neatly.

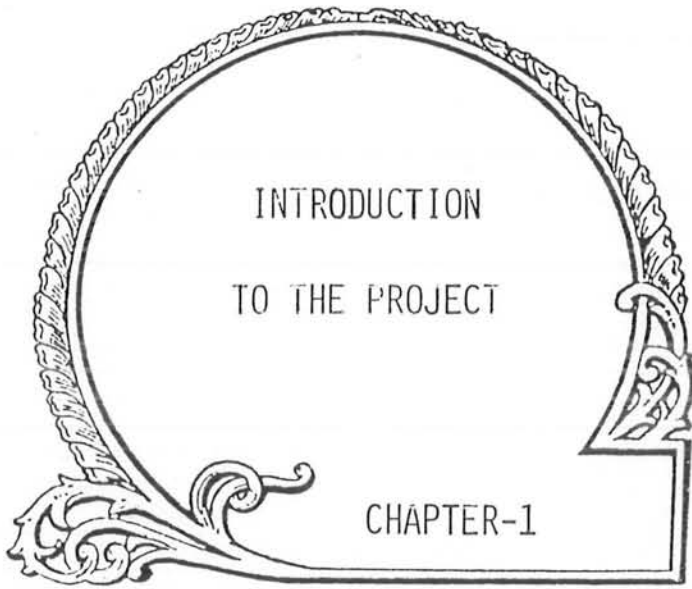
At the end, I lack vocabulary to pay tributes to Almighty Allah WHOSE constant help passed me through this task successfully.

MOHAMMAD ARSHAD



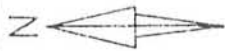
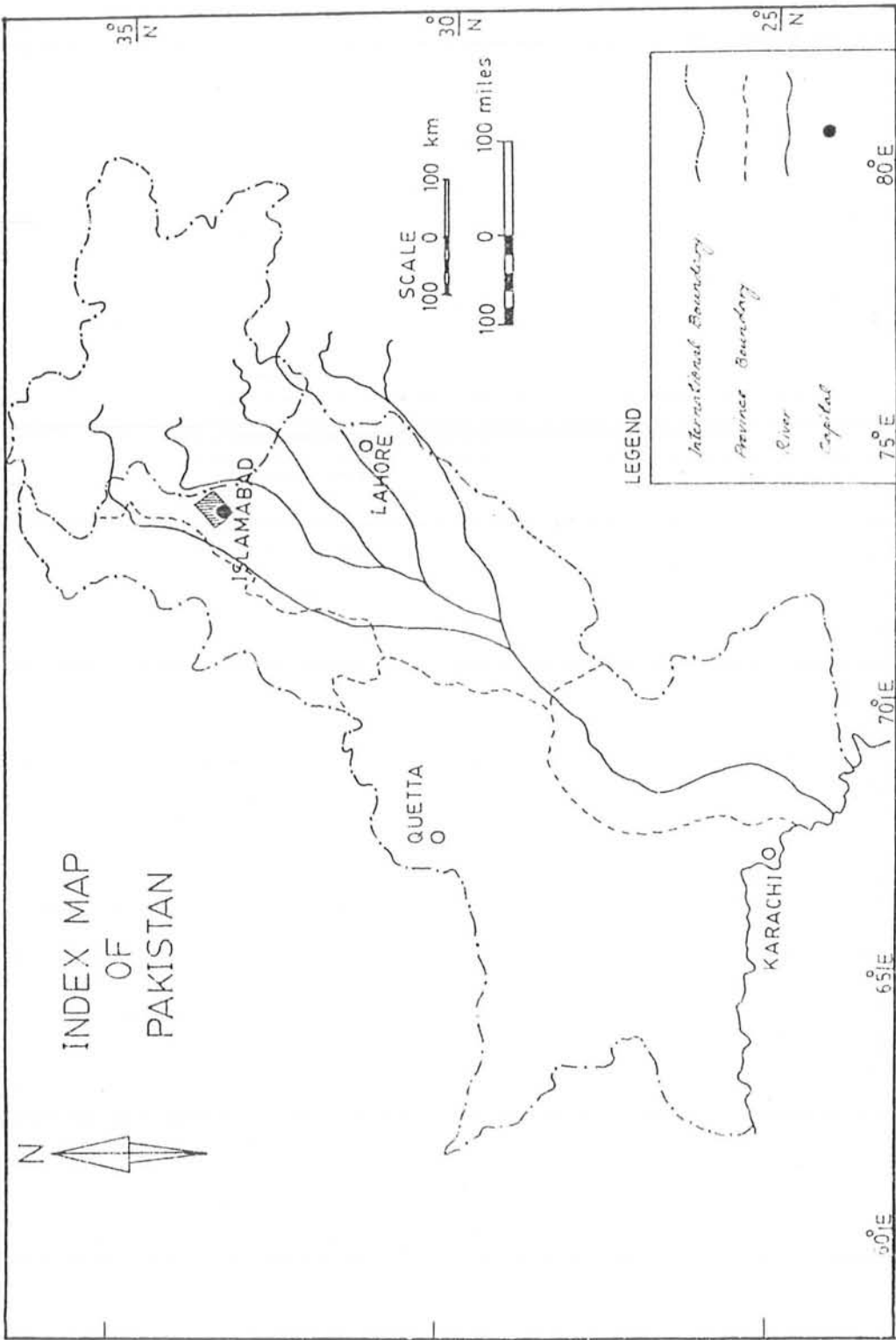
## ABSTRACT:

Gravity and magnetic studies were carried out on the western limb of Hazara Syntaxis for investigation of structural features. The basement trend revealed by regional gravity effects is in contradiction to the surficial geological structures which strike generally NE – SW and is similar to the model developed on the basis of earthquake seismology. It is envisaged that there exists a detachment zone beneath the investigated area. The basement seems to be dipping towards northeast at an angle of 2 degrees. The residual gravity effects associated with the overlying formations indicate that the Main Boundary Thrust extends from Margalla Pass to Ghoragali and Kuldana (Murree). A buried offshoot of the Main Boundary Thrust (MBT) is inferred to be passing near Mohra and Khanpur, and is exposed near Langrial and Nathiagali. Near Haripur, the maximum thickness of Holocene deposits over Hazara Slates is 400 metres.



INTRODUCTION  
TO THE PROJECT

CHAPTER-1

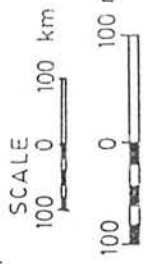


**INDEX MAP OF PAKISTAN**

35° N

30° N

25° N



ISLAMABAD

LAHORE

QUETTA

KARACHI

**LEGEND**

- International Boundary*
- Province Boundary*
- River*
- Capital*

75° E

70° E

65° E

60° E

80° E

## 1.1 INTRODUCTION:

The area investigated gravitationally and magnetically, discussed in this thesis, lies in the districts of Rawalpindi, Islamabad and Hazara. It is bounded by latitudes  $33^{\circ} 37'$  to  $34^{\circ} 10.1'$  N and longitudes  $72^{\circ} 37'$  to  $73^{\circ} 24'$  E, and spreads over toposheet numbers 43C/9, 43C/13, 43C/14, 43F/4, 43F/8, 43G/1, 43G/2, 43G/5 of Survey of Pakistan (Scale 1:50,000).

The gravity and magnetic observations were made in roughly 2500 square kilometres along the available metalled and unmetalled roads, at station interval of 1 to 2 km depending upon the topography. The profile density of one station per kilometre provides a fair control to fulfil the objectives of the survey.

Geologically the area comprises of predominantly sedimentary and less metamorphic rocks. In the south, tertiary sedimentary rocks of Murree formation are underthrusting the limestones of different ages from Eocene to late Jurassic (Iqbal & Shah, 1980). Whereas in the northern side, Precambrian Hazara slates are exposed on surface and are involved in thrusting with limestones (Coward & Buttler, 1985) mainly in the south and occasionally in the extreme north. Hazara formation is underlain by Lei Conglomerate at places particularly in the north-west frontier of the surveyed area.

The area is highly folded and faulted, and generally shows a structural complex controlled by the Hazara arc which is associated with the Main Boundary thrust (MBT) that developed due to a collision between the Indian and the Eurasian plates (Powell, 1979) about 60 Mya. The arcuate

trend of structures in the area is characterized by singly as well as doubly plunging folds with wavelength ranging from tens of metres to a few kilometres. Overall dip of the bedding planes is in the NW or SE direction.

Physiographically the area can be divided into low, medium and high relief units. The major proportion of the area lying along G.T. Road and Hareepur routes is generally plain with relief 450 m to 600 m, whereas the remaining hilly tract is of medium (Elevation  $\approx$  600 m) to high relief (Elevation  $>$  2500 m).

In the northern part vegetation is relatively thick and thins out towards south. Countless tributaries emanating from the elevated region of the area contribute to the evolution of hospitable environments and to the local terrain. Two major seasonal rivers flow through this area, the Haroo river in the Hazara district, and the Soan river in the Rawalpindi district.

## 1.2 PREVIOUS WORK:

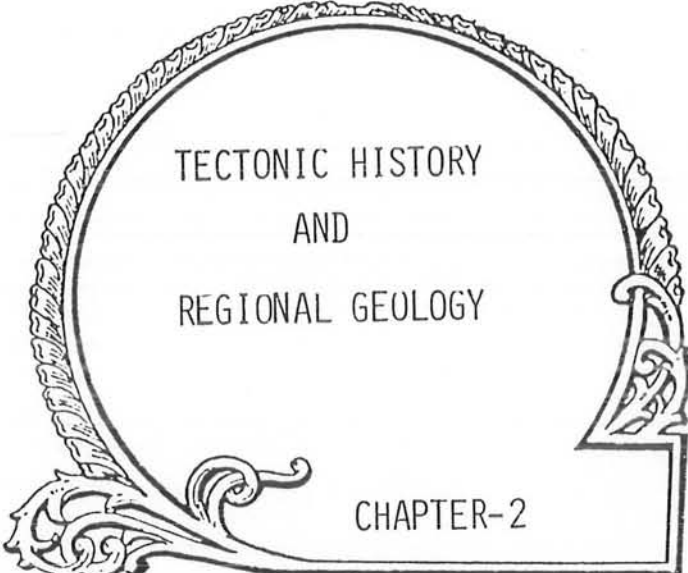
Previously, the area has been explored geologically by different workers with more emphasis on geological investigations rather than geophysical work. To explain the tectonic setup of the area, geological models have been constructed, based on information of surface lithologies (Latif, 1970; Coward & Buttler, 1985) and structural trends.

Geophysical work has not been done particularly in this area, however, references have been made in megascopic study of northern Pakistan based on regional gravity profiles and the earthquake data (Seeber & Armbruster, 1979). The results indicate that a seismically active zone is occurring at a depth of 12 to 20 km beneath Terbela, and may be a

downward projection of the Hazara fault (Seeber & Jacob, 1977).

### 1.3 FORMULATION OF THE PROJECT:

Since the area under investigation is a part of Himalayan arc, it defines an important example of the continental collision zone. The Main Boundary Thrust Zone (MBTZ) being a major tectonic feature has been attempted geologically (Coward & Buttler, 1985) and different views exist in literature. However, geological work has not been constrained properly by geophysics as such data are not available. Thus, the present project was formulated to provide sufficient geophysical control to previously existing geological ideas particularly about the Hazara Thrust System.



TECTONIC HISTORY  
AND  
REGIONAL GEOLOGY

CHAPTER-2

## 2.1 TECTONIC HISTORY:

The project area, covering approximately 2500 square kms, lies in the foothills of PAKISTAN Himalaya, where most of the geological features are thought to be the result of the collision of Indian plate with the Eurasian plate. Himalaya developed as a result of this event at the consumption of tethyan sediments in cretaceous times [Powell, 1979].

The main collision, of Indian plate with the Eurasian plate, occurred during late eocene which is predated, in cretaceous times, on Western Himalayan side because of trapped Kohistan Island Arc Complex [Windley, 1983]. At present Indian plate is subducting under the obducting Eurasian plate [Powell, 1979] due to northward drifting of Indian plate. This is observed through studying the results of deep seismic sounding surveys [Narain, 1979] and estimation of crustal thickness which is doubled in tibetan plateau region [Kono, 1974]. The resulting features, of described collision process of plates, include an extensive thrust system in the region which is marked by different geological structures as briefed below.

### a) Indus Suture Zone:

The Indus Tsangpo Suture zone or Indus Tsangpo Ophiolites mark the plate boundary between Indian and Eurasian plates which extends as a linear belt along Indus Tsangpo valley between Karakoram range in the north to Himalaya range in the south. It is best exposed for about 100 km in Ladakh region [Gansser, 1980]. In western Ladakh region, this single Suture zone is subdivided into two zones known as Main Mantle Thrust [MMT] in the south [Tahirkheli, 1978] and Main Karakoram thrust [MKT] in the



north [Bard, 1979]. The region between these two zones is called Kohistan - Island Arc sequence [Tahirkheli, 1978]. Regional Metamorphism is a characteristic feature of Ophiolite belt and associated sediments which is exhibited by greenschist facies [Frank et al, 1977] and flysch section with greenschist to amphibolite facies [Chang et al, 1977]. Typical rock, types associated with MKT on northern side are slates, quartzites, and metasediments while on the south serpentinite, basalt, andesite and rhyolite are present. Typical rock unit, associated with MMT, is glaucophane blue schist which separates basic complex of Kohistan from schistose rocks of Buner (lower Swat) [Tahirkheli, 1979]. The so called Kohistan-Island arc complex is composed of intermediate rocks like gabbros, diorites, metasediments (phyllites or shales) and volcanic rocks of Calc-alkaline nature (andesites, dacites, rhyolites, tuffs and agglomerates). The age of the Kohistan sequence ranges from cretaceous to paleocene [Tahirkheli, 1982].

b) Main Boundary Thrust Zone:

A significant fault called Main Boundary Thrust (MBT) lies in the south of Indus Suture zone as shown in figure 2.1 [Coward & Butler, 1985]. This thrust extends to a distance of 2500 Km along Himalayan range. A notable feature on western side of Himalayan mountain belt that is, PAKISTAN HIMALAYA, is a syntaxial belt associated with MBT. This is referred as Punjab Orocline [Casey, 1958], "Abbottabad syntaxis" [Jones, 1960], "Western Himalayan Syntaxis" [Gansser, 1964], the "Punjab Re-entrant" [Johnson & Vondra, 1972], the "Hazara Kashmir Syntaxis" [Calkins et al, 1975], "Hazara Syntaxis" [Desio, 1976], the "Jhelum Re-entrant" [Visser & Johnson, 1978]. The term "Hazara Syntaxis" is used by the author in this report.

To the western flank of Hazara Syntaxis, a system of local thrusts is associated called Hazara Arc [Seeber & Jacob, 1977] with a general trend being in the NE-SW direction as shown in figure 2.2. The rocks associated with MBT, of tertiary age, are sedimentary in origin consisting of loess, sandstones, limestones and shales.

c) Salt Range:

The Salt Range lies to the south of Main Boundary thrust separated by Potwar Plateau. It is divided into Salt Range and the Trans-Indus Salt Range, the latter including Marwat, Bhitani Surghar and Khisor Ranges. The Salt Range itself comprises of two bends, the smaller one being on the east and a larger one on the west, while the Trans-Indus Salt Range forms a Syntaxis on the western end of the Range as shown in figure 2.1. Tertiary sediments constitute the geological composition of the region.

2.2 REGIONAL GEOLOGY:

The area under investigation lies in the northern part of Indus basin consisting of sedimentary rock formations corresponding to non-uniform environments of deposition within trough (tethy sea) - the upper Indus basin.

In the adjacent north of the project area, the dominant rock types are igneous and metamorphic, of cambrian age, alongwith quartzite schists, quartzitic and schistose conglomerates. Rock units within the area are spatially distributed in the NE-SW direction and are of pre-cambrian age [Iqbal & Shah, 1980]. These rocks are composed of slates, phyllites and shales of Hazara formation [Iqbal & Shah, 1980] overlaid by conglomerate of Havelian group, of pleistocene age, which is widely exposed in the area. Other overlying sedimentary

formations include Abbottabad, Datta, Samana Suk, Chichali, Lumshiwai, Kawagarh, Hangu, Patala, Kuldana, Margalla Hill Limestone and Chorgali. These formations range in age from early jurassic to late eocene [Iqbal & Shah, 1980] and are composed of limestones, sandstones, siltstones, mudstones, conglomerates, quartzites and marls. The most important components are thinly bedded nodular dolomitic limestones with laterite bands and gypsiferous shales, both bearing a wide exposure. In the south sedimentary formations are prominently exposed between Nathiagali and Murree with an almost linear structural trend in the NE-SW direction. Typical rock units at and around Nathiagali are grey arenaceous and dolomitic limestones of Samana Suk formation, thinly bedded limestone along with intercalations of cleaved and calcareous shale of Kawagarh formation, grey nodular limestone with laterite bands of Hangu formation, patala shales, red and purple gypsiferous shales of Kuldana formation with subordinate sandstone and limestone bands and widely exposed Margalla Hill Limestone. These rocks extend to the south-west of the project area through Nathiagali and Kheragali along the structural trend as shown in figure 2.2.

---

From Kheragali towards Murree, the following succession of sedimentary rock formations is observed:-

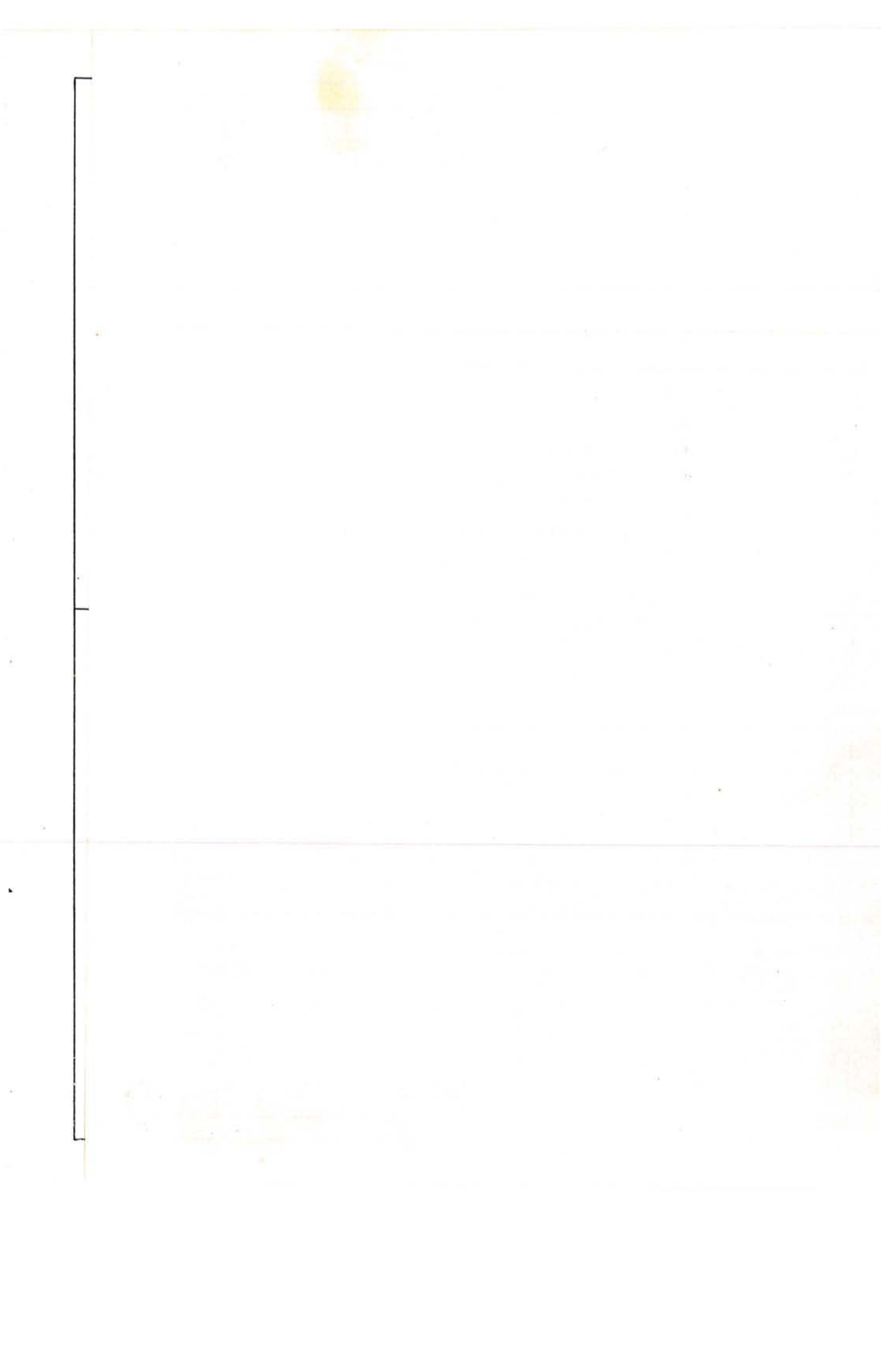
- i) Chorgali formation, of late eocene age, having limestone and shale.
- ii) Margalla Hill Limestone of eocene age.
- iii) Kuldana formation, of early eocene age, with red, purple gypsiferous shales, sandstones and limestones.

This composition also bears the same spatial distribution in the south-west quadrant of the project area, that is, along the structural trend of the rock formations.

On the south-eastern flanks of the area, Murree formation is prominent and composed of greenish grey sandstones and purple shales which is overlaid by the Havelian group, comprising gravels, loess, clay etc, being a distinct geological feature in the southern part. A sharp tectonic contact, between Murree formation and Margalla Hill Limestone is demarcated in the SE of the area, which diffuses to the south by the overlying conglomerates of Havelian group figure 2.2.

### 2.3 STRUCTURE:

Structurally the area under investigation is complex, showing multiphase deformational patterns resulting from the collision of Indian and Eurasian plates. Structures trending in the NE direction exhibit single as well as doubly plunging arcuate fold patterns. Major tectonic features in the area, as demarcated by surface lithologies, consists in generally of thrust faults of Hazara Thrust System with an overall dip of the thrust sheets in the NW direction. Wavelength of the folds in the area varies from tens of metres to several kilometres. Subsequent deformation in the area has resulted into the development of faults different from thrust system, e.g. dextral faults [Fig. 2.2].



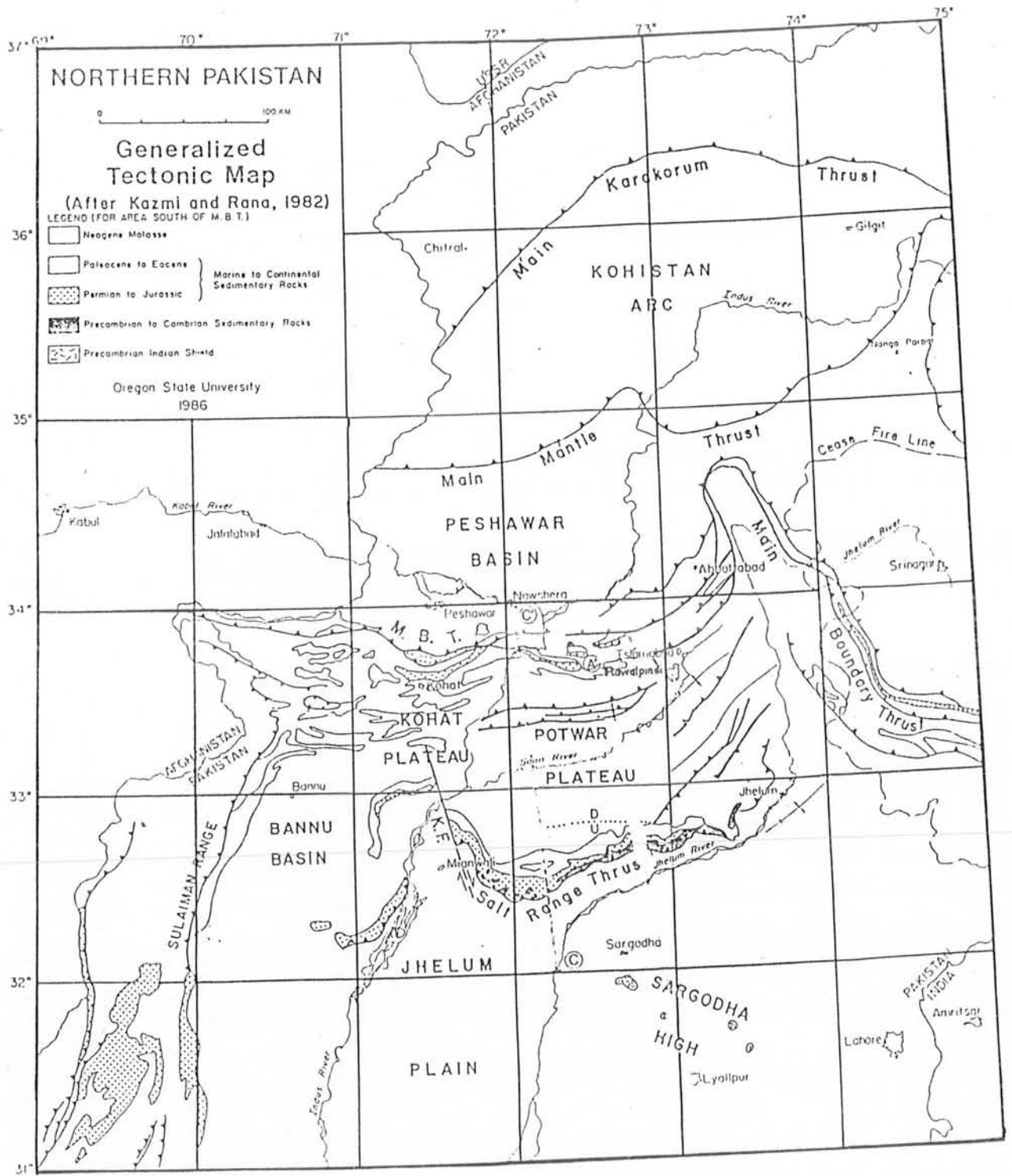

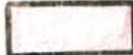




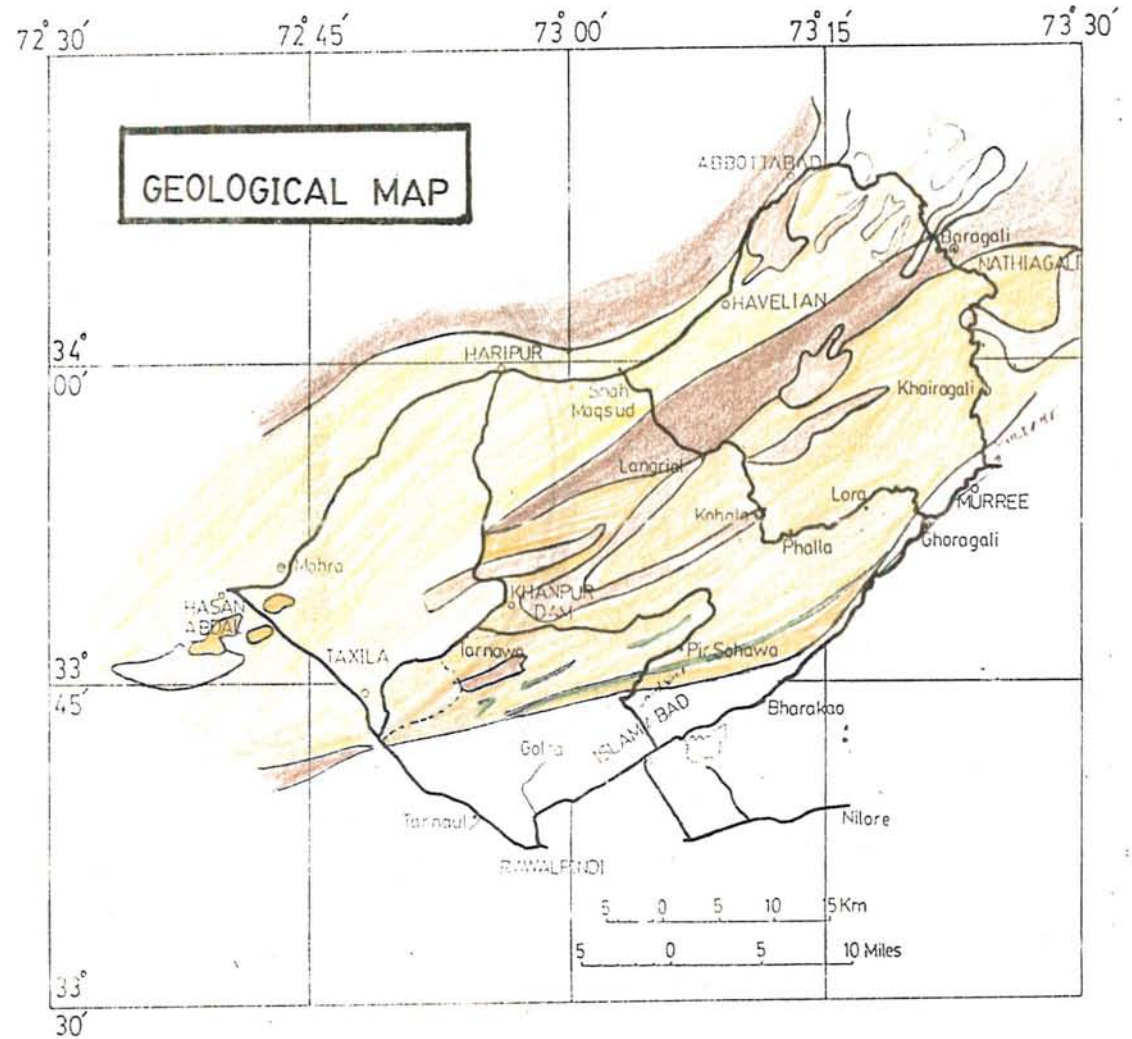


Fig. 2.1

**LEGEND:**

-  Recent Material
-  Miocene Sandstone
-  Paleocene/Eocene Limestone
-  Cretaceous Limestone
-  Jurassic Limestone
-  Pre-Cambrian Slates



### 3.1 GRAVITY PROSPECTING:

#### 3.1.1 Introduction:

Gravity prospecting involves measurement of earth's gravitational force which varies from equator to poles and can be predicted for any point fixed on the surface of the earth by the international gravity formula given below [Dobrin; 1976, p. 364]

$$g_{\phi} = g_e [1 + 0.0052884 \sin^2 \phi - 0.000059 \sin^2 2\phi] \quad \dots \quad (3.1)$$

where  $\phi$  = Latitude,  $g_e$  = gravity at the equator. Since the international gravity formula is based on the assumption that the earth is an ellipsoid of revolution having uniform density, the predicted value of gravity for a point would differ from the actual value due to deviations in topography and density from ideal conditions. The Newton's law of gravitation which provides the basis for the change in gravity, due to density and topography, is produced below for explaining its use in gravity prospecting

$$\text{i.e. } F = G \frac{m_1 m_2}{r^2} \quad \dots \quad (3.2)$$

$$\text{or } a = F/m_2 = \frac{Gm_1}{r^2} \quad \dots \quad (3.3)$$

If 'a' is replaced by 'g' (the gravitational acceleration),  $m_1$  by  $M_e$  (the mass of the earth) and 'r' by  $R_e$  (the radius of the earth) then

$$g = G \frac{M_e}{R_e^2} \quad \dots \quad (3.4)$$



In C.G.S. system, the unit of 'g' is  $\text{Cm/sec}^2$  and in geophysics it is called gal after Galileo. The average value of 'g' at the earth's surface is 980 gals, ( $1 \text{ gal} = 1 \text{ cm/sec}^2$ ), but actually it increases gradually from the equator (978 gals) to the poles (983 gals).

In gravity prospecting 'gal' is a very big unit, therefore, in exploration commonly used units are

$$\text{milligal (mgal)} = 10^{-3} \text{ gal}$$

$$\text{Gravity Unit (GU)} = 10^{-4} \text{ gal}$$

From equation (3.4) it is evident that the gravity is directly proportional to mass and inversely proportional to the square of distance between the centres of the earth and the point mass on the surface of the earth. This means that if there is a change in  $M_e$  or  $R_e$  'g' will vary accordingly. The dependence of 'g' on mass may be associated with density because mass of a body is the product of its volume and density. Thus 'g' is a function of density.

The density variations in the earth's crust are quite apparent because the upper crust is composed of a variety of rocks, ore deposits and mineralized zones of different densities. These density differences, therefore, are subjected to a change in gravity which is picked by sensitive instruments such as Eotvos Balance or the gravimeters.

Gravity prospecting is actually an indirect method where changes in gravity are interpreted in terms of subsurface density variations, to be modelled for solving geological problems or demarcating zones of economic minerals or hydrocarbons.

## 3.2 GRAVITY SURVEYS:

### 3.2.1 General:

The gravity surveys are commonly conducted to solve geological problems of regional or local level or to demarcate, from large areas, anomalous zones of economic value. In all these cases, the observed field gravity data is processed to compensate the gravity effects caused by the elevation differences of the gravity stations, surface irregularities and latitudinal changes from the fixed reference point taken in the surveyed area. The corrected gravity values of the stations when compared with the gravity value of reference point, some differences are found which technically are known as the Bouguer anomaly values. In gravity prospecting the investigated areas are represented by the Bouguer anomaly maps on which the nature of variation in Bouguer anomaly defines subsurface density changes or lithologic changes brought out by geological structures or localization of minerals. The magnitude of Bouguer anomalies expected in regional cases may be tens of milligals, where as in local surveys it may be a couple of milligals or less.

The Bouguer anomalies are obviously the function of independent variables like elevation, north-south distances and the surface density. Thus the accuracy of Bouguer anomalies is based on the accurate measurement of these independent variables. However, it is precautionary, particularly in local surveys that the error in Bouguer anomaly calculation should not exceed 25% of the expected magnitude due to causative sources of regional or local extent.

Generally there are three types of gravity surveys, reconnaissance, regional and local.

### 3.2.2 Regional Surveys:

Regional surveys are conducted over large territories in order to study large structures such as tectonic regions, continental margins or the basins. Since the expected anomaly in such cases is tens of milligals, the acceptable error may be a few milligals depending upon the magnitude of the anomaly. However, the situation can be improved by adjusting station network, taking appropriate density, reducing interstation distance and using small scale maps.

### 3.2.3 Reconnaissance Surveys:

Reconnaissance surveys are aimed at revealing structural trends, faults, large ore deposits etc. These depict more details than the regional surveys because of more dense network, less station interval and smaller scale maps, and are subjected to reduced error magnitude for giving enhanced reliability in the results.

### 3.2.4 Detailed Gravity Surveys:

These are precision gravity surveys which enable the demarcation of mineralized zones, oil and gas bearing structures and other local subsurface changes. Since the total anomaly expected in these surveys is a few milligals, the error magnitude should be the fraction of a milligal.

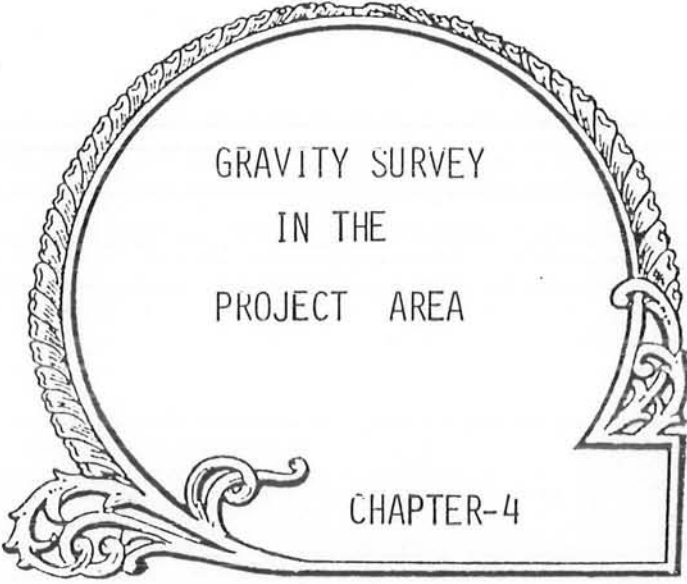
The table describing different parameters of each type of survey is given below [After Sazhina, 1971].

The survey can be carried out following the procedure of areal or profile surveys depending upon the objectives. The areal survey is best suited for interpreting three dimensional subsurface lithologic changes, whereas profile surveys are

Contour Interval	Scale of Map	Accuracy of Determn. of Bouguer Anomalies	Accuracy of Determn. of Observation	Network Density	
				Area per Station km <sup>2</sup>	Inter-Stn. Interval km
10	1:2,500,000 1:1,000,000	upto $\pm 2.5$	upto $\pm 0.3$	150 - 400	5 - 10
5	1:1,000,000 1:500,000	" $\pm 2.0$	" $\pm 0.3$	25 - 100	2.5 - 5
2	1:200,000 1:100,000	" $\pm 0.8$	" $\pm 0.3$	4 - 10	1 - 2
1	1:100,000 1:50,000	" $\pm 0.4$	" $\pm 0.3$	1 - 4	0.5 - 1
0.5	1:50,000 1:25,000	" $\pm 0.2$	" $\pm 0.15$	0.2 - 1	0.2 - 0.5
0.2 - 0.25	1:10,000 1:5,000	" $\pm 0.1$	" $\pm 0.08$	0.02-0.1	.05-0.15
0.1	1:5,000 1:2,000 1:1,000	" $\pm 0.04$	" $\pm 0.03$	0.002-.01	.02-.05

Table: Characteristics of Gravity Surveys.

conducted along separate routes with wider profile intervals to study a unidirectional variation of gravity. Nevertheless, profile surveys are valuable tool to explore rugged terrains to find out tectonic patterns, local and regional structural trends etc.



GRAVITY SURVEY  
IN THE  
PROJECT AREA

CHAPTER-4

#### 4.1 GRAVITY SURVEY IN THE PROJECT AREA:

##### 4.1.1 General:

As mentioned earlier the project area, which lies between Islamabad, Murree and Abbottabad, comprises of low and high relief segments. In the later part except for the metalled roads, the jeepable tracks are very short and rare. Therefore, gravity investigations in the whole area were made along the main routes. In that sense, the survey can be described as the profile survey. However, an attempt was made to establish a network of gravity stations in the area. In plain area the station interval was selected 1 Km, whereas in rugged terrain it was increased from 1.5 to 2.0 Km to maintain consistency in the station interval. Contrarily, consistency in profile interval could not be established due to inaccessibility of difficult terrain and shortage of time. It is quite obvious that in this approach many local geological features may not be scanned but no risk is involved as far as the larger features are concerned. The major profiles are oriented along and across the strike to cover neogene to cambrian sequence of the areal geology.

#### 4.2 FUNCTION OF WORDEN GRAVIMETER:

The Worden Gravimeter which was used for measuring gravity variations in the area is an unstable type portable gravimeter (Dobrin, 1976, P-386). This is able to measure relative gravity changes in the area with respect to a fixed point, generally Main Base of known gravity, rather than the absolute gravity values of observed stations.

The readings obtained are in terms of scale divisions which on multiplication with scale constant of the gravimeter (1 S.D. = .0902 mgals) are converted into

milligals. The maximum range of the gravimeter is 2300 scale divisions or 207.46 mgals. which could be used in an area of maximum elevation change less than 800 meters (discussed in Section 4.6.4). If elevation changes are more than 800 meters or multiple of 800 m then the gravimeter needs to be recalibrated on some stations, known as auxiliary bases, for covering other ranges.

The gravimeter is provided with recalibration facility and is thermally compensated for external temperature variations from  $-20$  to  $+95^{\circ}\text{F}$ . As the internal system of the gravimeter is mechanical, it shows a minor hysteresis with time the effect of which included in gravity observations is compensated later while data processing.

#### 4.3 ESTABLISHMENT OF BASE STATION:

##### 4.3.1 General:

The gravimeters of Wor-  
don type are incapable of measuring absolute gravity at a point taken on the earth's surface but measure differences with respect to a point of known absolute gravity value by setting the range appropriately to account for the elevation effect. Hence, it is necessary to establish a base station in the field before starting a survey. If the area under investigation is too large and lies in a rugged terrain then the limitation of time and the range of gravimeter restricts the survey to a particular elevation range or to a certain distance from the base station. To overcome these difficulties, auxiliary base stations are established in the area which in turn are tied to the main base station so that the observed data of the whole area may be reduced eventually with respect to the main base station.

4.3.2 Establishment of Zero-Point (Islamabad)  
as Main Base:

The main base of the project area was selected at half a kilometer in the east of overhead bridge of Zero Point (Islamabad), located at the junction of Kashmir Road and the offshoot linking the Islamabad Highway. The latitude and longitude of the Base Station are 33.0313375 degrees North, and 73.0722761 degrees East respectively. This was tied to an International Gravity Station, by Looping Method, located in the Christ Church (Rawalpindi) with latitude and longitude being 33.58889 North and 73.05 East meridian respectively.

4.3.3 Computation of Absolute Gravity at the Base:

For determining absolute gravity value of the Main Base Station several gravimeter readings were taken on the selected base and at Christ Church (Rawalpindi). The average gravimeter readings on both the stations are:

Zero-Point	2131.5 Scale Divisions
Christ-Church	2202.0 " "

The difference between these values is 67.4 scale divisions which becomes 6 mgals on multiplication with the scale constant of the gravimeter (i.e. 0.0902). If the gravimeter reading at the Church, i.e. 2202 scale divisions, corresponds to the known absolute gravity value at the Church (979350.3 mgals), then the absolute gravity value at Zero-Point appears to be equal to

$$979350.3 - 6.0 = 979344.3 \text{ mgals.}$$



4.3.4 Auxiliary Base Stations:

As mentioned earlier it was not possible to investigate the whole area by single gravity calibration. The area was divided into four segments and the following four auxiliary bases were established as described below:

STATION	ABS. GRAVITY (mgal)	ELEVATION (ft.)	LOCATION	
			<u>Latitude</u>	<u>Longitude</u>
Mohra	979381.2	1474	33°50'28"	72°44'2"
Ghoragali	979152.3	4956	33°52'55"	73°20'29"
Khairagali	978984.0	7601	33°59'38"	73°23'43"
Baragali	979100.6	5833	34°5'35"	73°21'27"

#### 4.4 ACQUISITION OF GRAVITY DATA:

##### 4.4.1 Procedure:

As mentioned earlier the gravity value of a point on the earth's surface is a function of elevation, latitude and the density, in gravity prospecting therefore, all these values are needed alongwith the gravity observations of the stations established in the field. Generally surface density of the area is assumed to be constant, whereas the latitudinal variations are found from the toposheets of the area. Thus, in the field, gravity observations of the stations are accompanied by elevation observations.

The elevation in the studied area varies widely from roughly 600 m to 3000 m and in this range the expected gravity variation is larger than the range of the gravimeter. This situation raised the necessity of dividing the area into zones of different elevation ranges (600 - 1400 m, 1400 - 2200m, 2200 - 3000 m.) and in each zone one auxiliary base was established. These auxiliary bases, later on, were linked with the main base.

In the surveyed area a network of observation stations was established along the metalled roads with a station interval of 1 Km in plain region and 1.5 to 2 Km in rugged terrain. As there are not too many roads or jeepable tracks in the area, the profile interval is much larger also. The measurements of gravity and elevation were followed profile by profile. Each profile of a zone was started from the base and ended with its repetition. The base repetition was done for the compensation of gravimeter drift which appears with time.

#### 4.4.2 Acquisition of Altimeter Data:

##### General:

The elevation of gravity stations play very important role in reducing the gravity data to a datum plane passed through the area, and in deciding the quality of interpretation. Thus, the precise information of elevation of the observation stations is highly needed to improve the reliability of results. Theoretically, the accuracy in measuring the elevations should be better than one meter. This error in elevation is equivalent to an error of 0.2 mgal (with density 2.67 g/cc) in the observed gravity of a point, which may not be acceptable sometimes in areas of low gravity anomalies or in mineral exploration ( $< 1$  mgal). Greater accuracy can be achieved with theodolites in altimetry but this is a slow procedure and reduces the surveying efficiency enormously particularly in rough terrains. However, a reasonable compromise between accuracy and efficiency can be had, in areas of large anomaly, with barometric type altimeters which have an accuracy of  $\pm 5$  ft, producing an error of 0.3 mgal in gravity (with density = 2.67 g/cc.). Normally a pair of altimeters is used, one placed at the base station for regular monitoring of the barometric changes (as a function of time) in the area, whereas the other is taken to the field to measure elevations of the gravity stations. These altimeters are capable of measuring elevations from -900 to +9700 ft, and are commonly used in gravity surveys.

#### 4.4.3 Data Collection:

For collecting elevation data, two American Paulin System (model PAB-5) altimeters, having a measuring range from -900 to +9700 ft with a precision of  $\pm 5$  ft, were used.

One of them was set in the middle of the traverse, to record regularly the barometric changes at an interval of 15 minutes, while the other was taken to the field, alongwith the gravimeter, for measuring the heights of gravity stations above sea-level. Before start of the survey both the altimeters were calibrated to the known elevation of the base station and were operated as instructed in the manual supplied by the manufacturer. On each station the altimeter was exposed for a while before taking reading so that it may reach equilibrium state in present environment and was also protected from the impact of direct sun rays to avoid temperature fluctuations.

#### 4.5 REDUCTION OF ALTIMETER DATA:

##### 4.5.1 General:

Basically an altimeter is a barometric instrument which measures elevation as a direct interpretation of weight of air column above it. So its performance is affected by temperature and pressure changes in the surrounding atmosphere. In order to remove noise factors from observed data, caused by temperature and pressure changes, generally two types of corrections are applied: temperature correction and barometric correction.

##### 4.5.2 Temperature Correction:

The dial of the altimeter is calibrated for a temperature of  $50^{\circ}\text{F}$ , i.e. it will measure true differences in attitude at this mean air temperature (assuming no change in barometric pressure other than in altitude). When the average temperature of two consecutive stations falls below  $50^{\circ}\text{F}$ , the weight of the air column measured is then greater than the weight of the "standard" column (at  $50^{\circ}\text{F}$ ) and the altimeter will indicate a difference in attitude greater than the true

difference. When the average temperature is above 50°F the air column will be less dense than the "Standard" column and the measured difference in altitude will be less than the true difference. The temperature correction takes the same sign as the difference in altitude when the average temperature is above 50°F. But when the average temperature falls below 50°F the sign of temperature correction will be opposite to that of difference in altitude. This is calculated by computing percentage correction for a temperature above or below 50°F using the following formula:

$$\text{Percentage} = (T_1 + T_2 - 100) \times 0.102$$

In above formula, the average of two successive temperature readings  $T_1$  and  $T_2$  is used to obtain a close approximation of the temperature of air column being measured. By multiplying the percentage factor with the uncorrected difference in altitude, the temperature correction (in feet) is obtained.

#### 4.5.3 Barometric Correction:

The temperature corrected altimeter data retain the effects of atmospheric pressure changes of regional or local level which are to be compensated by applying the barometric correction.

The barometric correction could be supposed linear when the survey is conducted with one altimeter and traverses are of short duration (2 or 3 hours). But, when two altimeters are operated the base-altimeter provides accurate estimates of the barometric correction for the whole day, and this method allows long working hours. Through the study of base-altimeter record, it was observed that the major curvilinear changes in atmospheric pressure are overridden by minor sinusoidal changes and can not be predicted precisely by mathema-

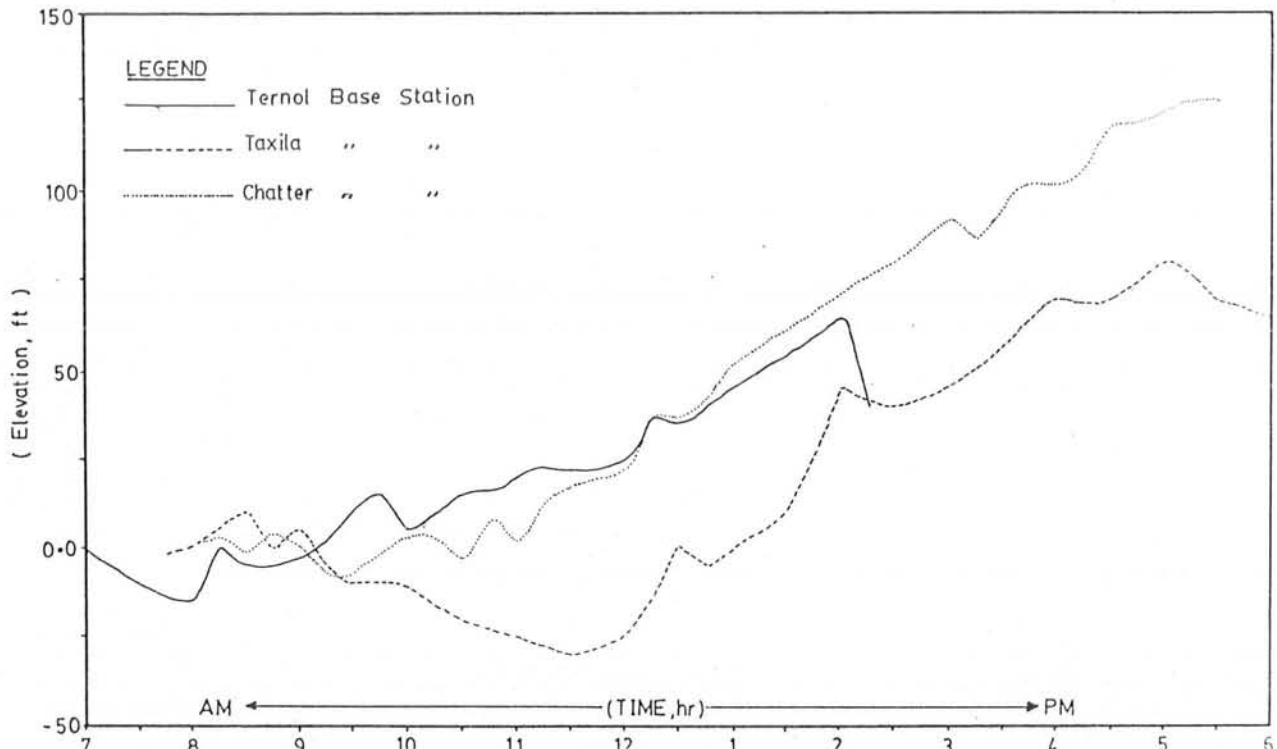


Fig. 4.1: Altimetre behaviour curves throughout the day obtained at different locations.

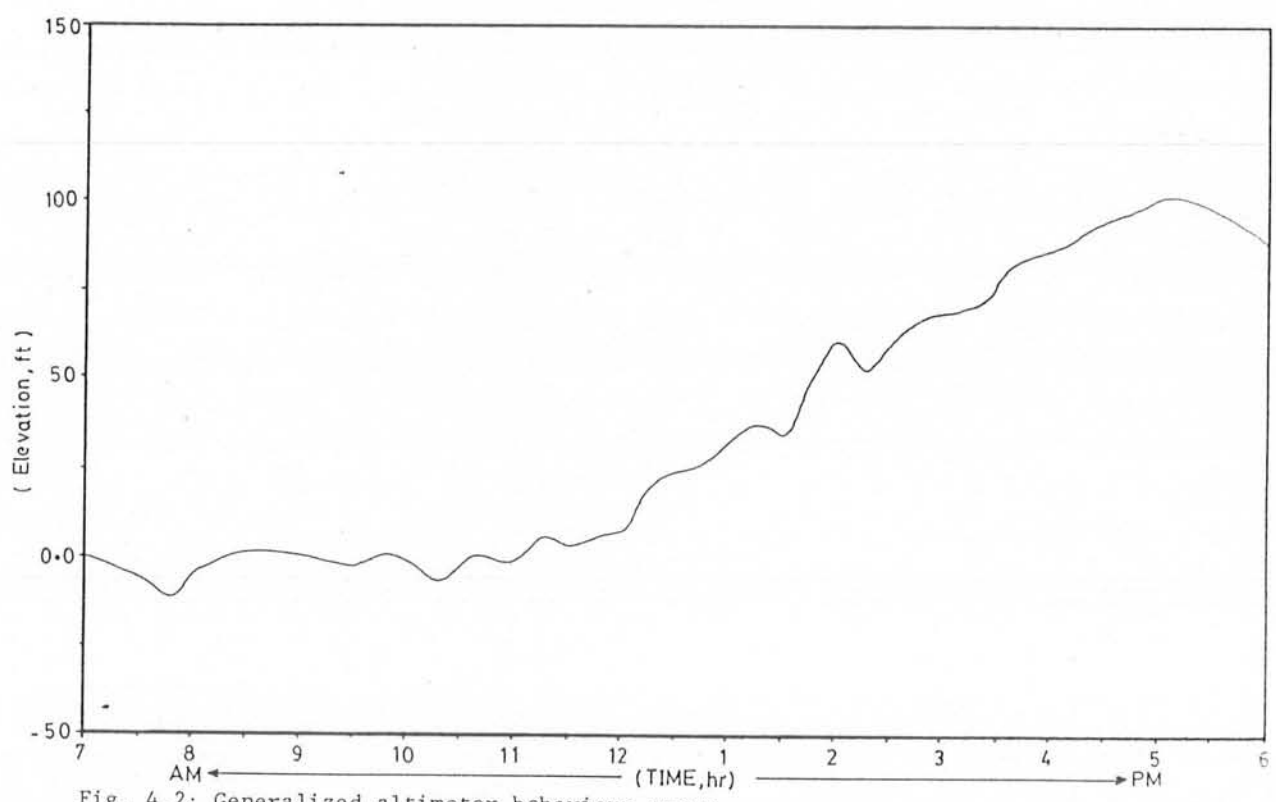


Fig. 4.2: Generalized altimeter behaviour curve.

tical models. Therefore, it is advisable to use two altimeters to achieve better accuracy in altitudes.

In the present survey, two altimeters were used to measure elevation of gravity stations. The behaviour of the base-altimeter is shown in the Figure 4.1. It can be observed that almost linear rise in altitude takes place between 10.00 A.M. to 5.00 P.M. but outside this time period the changes are different.

For recovering the nature of barographic correction at different times of the day, the temperature corrected base altimeter data was plotted against times of observations (Fig. 4.1). This curve was used to correct the temperature corrected field altimeter data of the same day, i.e. the correction factor, estimated from the curve for different times of observations in the field, was subtracted from the temperature compensated field altimeter data. This procedure was adopted for all traverses of long durations. The traverses for which base altimeter data was not available, a generalized altimeter behaviour curve (Fig. 4.2) was constructed for the field session and used carefully.

#### 4.6 REDUCTION OF GRAVITY DATA:

##### 4.6.1 General:

The observed gravity data involves the effects generated by instrumental drift, Latitudinal change in gravity, variation in elevation, subsurface density and surrounding terrain. To make the data interpretable it is necessary that the mentioned effects be removed carefully. For that purpose a datum plane is passed through the area, preferably sea-level in regional survey, and the observed data is reduced

to that plain giving gravity anomaly known as Bouguer anomaly. Mathematically Bouguer anomaly is given by

$$\Delta g = g_{ob} + D.C. + E.C + T.C. - T.G$$

where  $\Delta g$  = gravity anomaly

$g_{ob}$  = observed gravity

D.C = drift correction

E.C = elevation correction

T.C = terrain correction

T.G = Theoretical gravity

Except observed gravity ' $g_{ob}$ ', all the values in above equation are corrections detailed as follows.

#### 4.6.2 Drift Correction:

This correction removes the effect of instrumental drift, which appears with time in the instrument due to hysteresis phenomenon. If it is assumed that the drift is linear then it can be calculated simply by considering the initial and final gravity values of the base and respective time of those observations.

For removing the drift effect from the observed gravity of a point, the drift rate is multiplied with the time difference (=time of observation-time of observation at the base).



#### 4.6.3 Latitude Correction:

This correction is meant for latitudinal variation in gravity caused by earth's rotation, as discussed by Dobrin, 1976 p-420, and after application of correction, data is reduced on latitude of base station.

The usual way of applying latitude correction can be overlooked by computing theoretical gravity at each observation station which is subtracted from absolute gravity of the observed point to render gravity anomaly. International gravity formula to compute theoretical gravity is

$$g_{\phi} = g_e (1 + B \sin^2 \phi - C \sin^2 2\phi)$$

or  $g_{\phi} = g_e + B\phi \sin^2 \phi - C\phi \sin^2 2\phi - 951$

where  $\phi$  is latitude of observation station and  $B\phi$ ,  $C\phi$  are constants. While a constant term of 979000 mgals is subtracted from theoretical gravity as well as absolute value of gravity to avoid big figures in calculations.

#### 4.6.4 Elevation Correction:

The purpose of elevation correction is to adjust the computed value of gravity at the datum level. It comprises of two types.

- i) Free-air Correction.
- ii) Bouguer Correction.

##### i) Free-air Correction:

It takes care of the elevation effect upon the observed readings, discussed by Dobrin, 1976, p-417, so

that the data is brought on the datum level.

The correction is calculated by multiplying the correction factor ( $= .09406 \text{ mgal/ft}$ ) with the elevation difference between station and datum. This correction is added if observed point is above the datum and subtracted when below it.

ii) Bouguer Correction:

It is applied to compute the effect of idealized mass layer between station and datum plane. It is also calculated by (multiplying a constant factor ( $= .012776 \times \rho \text{ mgal/ft}$ ) with the elevation difference between observed point and the datum level. Where ' $\rho$ ' is density of idealized mass layer.

The theoretical derivation of Bouguer correction is described by Dobrin, 1976, p-417. The sign of Bouguer correction is opposite to that of Free-air correction.

4.6.5 Terrain Correction:

This correction compensates the effect of irregular terrain in the vicinity of observation station, that is, hills rising above the station and valleys below it. Both of these topographic undulations cause an effect in the same sense, reducing the observed gravity value due to upward pull (hills) or lack of downward attraction (valleys). Therefore, terrain correction is always added to the observed reading.

For removing terrain effect a digital computing method is adopted which developed by Bott (G.P., 1958, p-45).

The computer method for evaluation of terrain correction is simply automation of graphical method of Hammer [Dobrin, 1976 P-419] .

The maximum area covered, in the vicinity of observation station, to compute terrain effect is 16 Km which is equivalent to computing terrain correction upto zone L in case of graphical technique.

#### 4.7 CALCULATION OF CRUSTAL THICKNESS:

The thickness of the crust can be calculated from Bouguer anomaly data using empirical relations as given below:

$$Z = 33 - 0.055 \Delta g \quad (\text{Worzel \& Shurbet, 1955})$$

$$Z = 30 - 0.1 \Delta g \quad (\text{Andreev, 1958})$$

$$Z = 32 - 0.08 \Delta g \quad (\text{Woollard, 1959})$$

where Z is the crustal thickness in kilometres and  $\Delta g$  the gravity anomaly in milligals.

These relations have been picked out of a number of formulae because of the reason that they give almost similar answers. For calculating the thickness of the crust at a particular point, the averaged value is considered to be the best answer. Estimates of crustal thickness provide a useful information to think about the configuration of Moho discontinuity.

The application of these relations to our data give crustal thickness 46 to 49 kms, increasing towards northeast.

#### 4.8 ESTIMATION OF ERRORS:

For estimating error involved in this gravity survey, the following considerations were made:

##### 4.8.1 Error Due to Inaccurate Heights:

Heights of the field stations with respect to mean sea level were recorded with the altimeter within an error of  $\pm 5$  ft. Since the field altimeter data involve temperature and barometric effects, the temperature and barometric corrections were applied carefully using the data of other altimeter placed at a point in the middle of a profile. It was observed that the corrected heights have an error of  $\pm 5$  ft. For a density of 2.67 gm/cc used for Bouguer Correction, the gravity error due to  $\pm 5$  feet error in heights is equal to  $(\pm 0.09406 \times 5 \mp 0.012776 \times 2.67) = 0.3$  mgal.

##### 4.8.2 Error Due to Inaccurate Horizontal Control:

The maximum error involved in making stations is roughly 100 ft, which produces latitude gravity error

$$1.307 \sin^2 \phi \times \frac{100}{3 \times 1760} = 0.02 \text{ mgal.}$$

##### 4.8.3 Error Due to Inaccurate Density:

This error is introduced in the calculation of Bouguer Correction due to inaccurate determination of surface density of the area. Since the average density for sandstone, limestones and slates is 2.64, 2.69 and 2.53 respectively in the area, and the average crustal density 2.67 gm/cc used for Bouguer Correction is subjected to an

error of 0.05 gm/cc. The Bouguer reduction error thus obtained,

$$0.012776 \times 0.05 \times 1 = 0.0006385 \text{ mgal/ft.}$$

The mean height of the area above sea level is 4870 ft, therefore, the mean error of gravity anomaly is

$$\pm 0.0006385 \times 4870 = \pm 3.11 \text{ mgal.}$$

#### 4.8.4 Observational Error:

This is introduced while taking a reading and equals roughly 1/10th of a scale division of the dial, i.e., 0.01 mgal.

#### 4.8.5 Error Due to Inaccurate Base Connection:

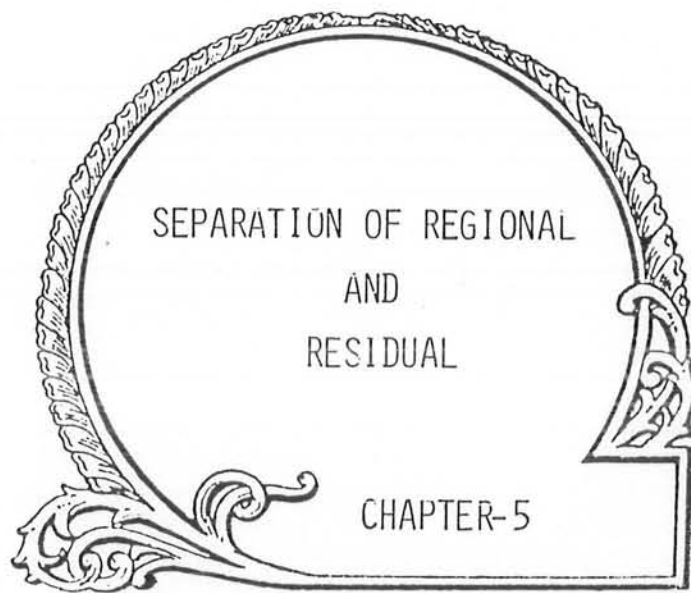
As mentioned earlier, the measuring range of the Worden Gravimeter is limited, i.e. 207 mgals. Thus, the area with relief 500 m to 2500 m could not be surveyed with a single calibration. Therefore, it became necessary to establish four auxiliary base stations (Section 4.3). Three check points were selected in the area which were investigated through two auxiliary bases, i.e. Station No. 78 (Haripur) was approached from Main Gravity Base Zeropoint (ISD) and Auxiliary Base Mohra and the difference of the two readings was noted 0.06 mgal. Similarly Stn. 89 (Shah Maqsud) was approached from auxiliary bases Mohra and Ghoragali and the error was found to be 0.25 mgal, Station No. 113 (Abbottabad) was approached through auxiliary bases Mohra and Baragali and the error was calculated roughly 0.87 mgal. The last check point is showing relatively large error probably due to two interconnections between Baragali and the Main Gravity Base at Zeropoint (ISD), and three times setting of the gravimeter. The average error emerged due to base connections is, therefore,  $\pm 0.4$  mgal.

4.8.6 Overall Accuracy Of The Gravity Survey:

The overall inaccuracy in the determination of Bouguer anomaly is root-mean-square of the errors involved.

$$\begin{aligned} \text{R.M.S.} &= \pm \sqrt{(0.3)^2 + (0.2)^2 + (3.1)^2 + (.01)^2 + (0.4)^2} \\ &= 3 \text{ mgals.} \end{aligned}$$

The error of 2 to 3 mgals is quite large, but if compared with the magnitude of the Bouguer anomaly in the area (170 to 210 mgals), it appears to be tolerable ( $\pm 7.0\%$ ) and the accuracy of this Gravity survey is well over 90 percent.



SEPARATION OF REGIONAL  
AND  
RESIDUAL

CHAPTER-5

## 5.1 SEPARATION OF REGIONAL AND RESIDUAL ANOMALIES:

### 5.1.1 Introduction:

The Bouguer Gravity values represent the combined effect of both the deep and shallow structures lying beneath the point of observation. Thus the interpretation of anomalies need to be resolved into regional and residual effects. Regional effects, caused by large scale structures such as a basin or a geosyncline, often obscure the effects of overriding shallower small scale structures such as salt domes or buried ridges etc. That is why, regional effects are separated from the observed gravity anomaly in order to project smaller features of interest. For separation of these effects commonly used procedures may be categorised as follows:

#### a) Graphical Methods:

Graphical approach requires a considerable skill of judgement in estimating regional effect from plotted profiles or contoured gravity anomaly maps. Regional contours are interpolated more or less arbitrarily from the original gravity field in the light of available geological information.

Though graphical technique is an easier way of separation of anomalies but it involves greater risk of misjudgement and misinterpretation.

#### b) Analytical Methods:

With analytical techniques residual and regional gravity effects are separated more precisely through numerical



operations and this could be done by four ways mentioned below;

- i) Centre-point and ring method
- ii) Second derivatives
- iii) Polynomial fitting or trend Surface Analysis
- iv) Downward Continuation.

For reliable separation the basic requirement of all these techniques is gridded data, whereas, the field data is oftenly collected over widely spaced profiles. In that situation an (linear) interpolated gridded data may be prepared, and polynomial fitting technique is considered suitable for separation of regional and residual anomalies. In the present case, polynomial fitting or trend surface analysis technique was selected because of the reason that the data was collected from irregularly widely spaced profiles.

#### 5.1.2 Trend Surface Analysis:

Trend analysis is a term used, generally, to define the concept of recovering regional trends from two-dimensional data. Application of this method depends particularly upon the size of the region being investigated and the size/nature of collected data. For example, it is useless to search meaningful local features whose expected size is less than the distance between sample points. The application of trend surface analysis on Bouguer anomaly data is based on the consideration that the Bouguer anomaly values are linear function of the geographic co-ordinates of the points of observation. This actually is a method to pass, mathematically, a best fitted plane of regression through the

observed data; this plane is regarded as regional trend or effect, whereas the deviations of observed data from this plane of regression are called the local or residual effects.

A first-degree polynomial passed through one-dimensional data, like that of a profile, produces a straight line which could be defined by the following relation.

$$\sum_i Y = b_0 + b_1 \sum_i X \quad (\text{where } i=1, n) \quad \dots \quad (5.1)$$

where  $b_0$  and  $b_1$  are unknown coefficients to be calculated,  $X$  and  $Y$  are independent and dependent variables respectively. This equation expanded over two independent variables, like co-ordinates of observed points, defines linear trend surface through the data.

$$Y = b_0 + b_1 X_1 + b_2 X_2 \quad \dots \quad (5.2)$$

where  $Y$  is the regressed Bouguer anomaly depending upon the co-ordinates  $(X_1, X_2)$  of observed points, as a linear function of some constant value ( $b_0$ ) related to mean of the observations plus an east-west ( $b_1$ ) co-ordinate component and the north-south ( $b_2$ ) component. Since there are three unknowns involved in the equation (5.2), we need three normal equations to estimate their values.

As a matter of fact the calculated Bouguer anomaly values, for the observed points in the area, produce a set of simultaneous equations given below

$$\begin{aligned} \sum Y &= b_0 n + b_1 \sum X_1 + b_2 \sum X_2 \\ \sum X_1 Y &= b_0 \sum X_1 + b_1 \sum X_1^2 + b_2 \sum X_1 X_2 \quad \dots \quad (5.3) \\ \sum X_2 Y &= b_0 \sum X_2 + b_1 \sum X_1 X_2 + b_2 \sum X_2^2 \end{aligned}$$

In matrix form above relations could be defined as follows,

$$\begin{bmatrix} n & \Sigma X_1 & \Sigma X_2 & b_0 \\ \Sigma X_1 & \Sigma X_1^2 & \Sigma X_1 X_2 & b_1 \\ \Sigma X_2 & \Sigma X_1 X_2 & \Sigma X_2^2 & b_2 \end{bmatrix} = \begin{bmatrix} \Sigma Y \\ \Sigma X_1 Y \\ \Sigma X_2 Y \end{bmatrix} \dots \quad (5.4)$$

This matrix of the form  $AX = Y$  can be solved for  $A(b_0, b_1, b_2)$  using the principle of linear simultaneous equations. With the knowledge of these constants and independent variables ( $X_1, X_2$ ), the regressed Bouguer anomaly values ( $Y$ ) could be estimated for the observed points. The plot of these values would give a linear trend surface or produce a linear Regional gravity effect, whereas the deviations in the observed values ( $Y$ ) from those of the estimated values ( $\bar{Y}$ ) reveal the Residual gravity effect (associated to local or shallower features).

If the first-degree solution does not provide best fit to the observed data, then analysis is required in which each geographic co-ordinate is simply raised to a higher power to include new variables. For example, a second-degree trend surface is defined by expansion of equation (5.2)

$$Y = b_0 + b_1 X_1 + b_2 X_2 + b_3 X_1^2 + b_4 X_2^2 + b_5 X_1 X_2 \dots \quad (5.5)$$

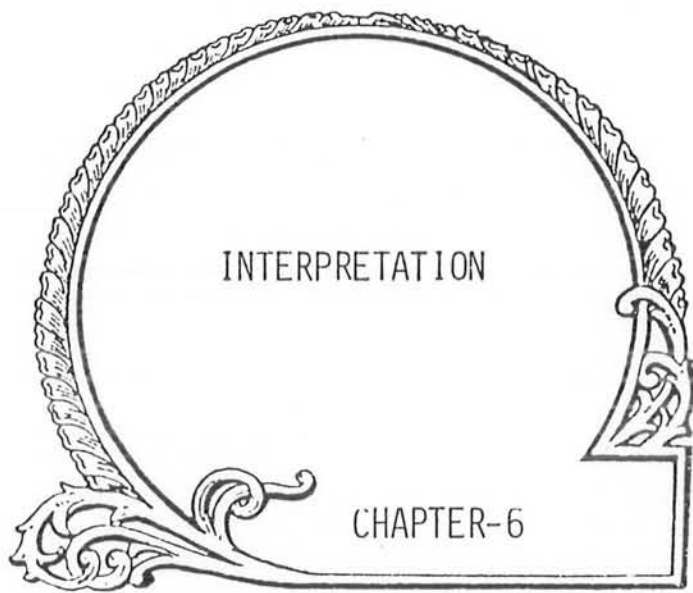
Similarly, third-degree trend surface equation is

$$Y = b_0 + b_1 X_1 + b_2 X_2 + b_3 X_1^2 + b_4 X_2^2 + b_5 X_1 X_2 + b_6 X_1^3 + b_7 X_2^3 + b_8 X_1^2 X_2 + b_9 X_1 X_2^2 \dots \quad (5.6)$$

### 5.1.3 Application of trend surface analysis to Present Case:

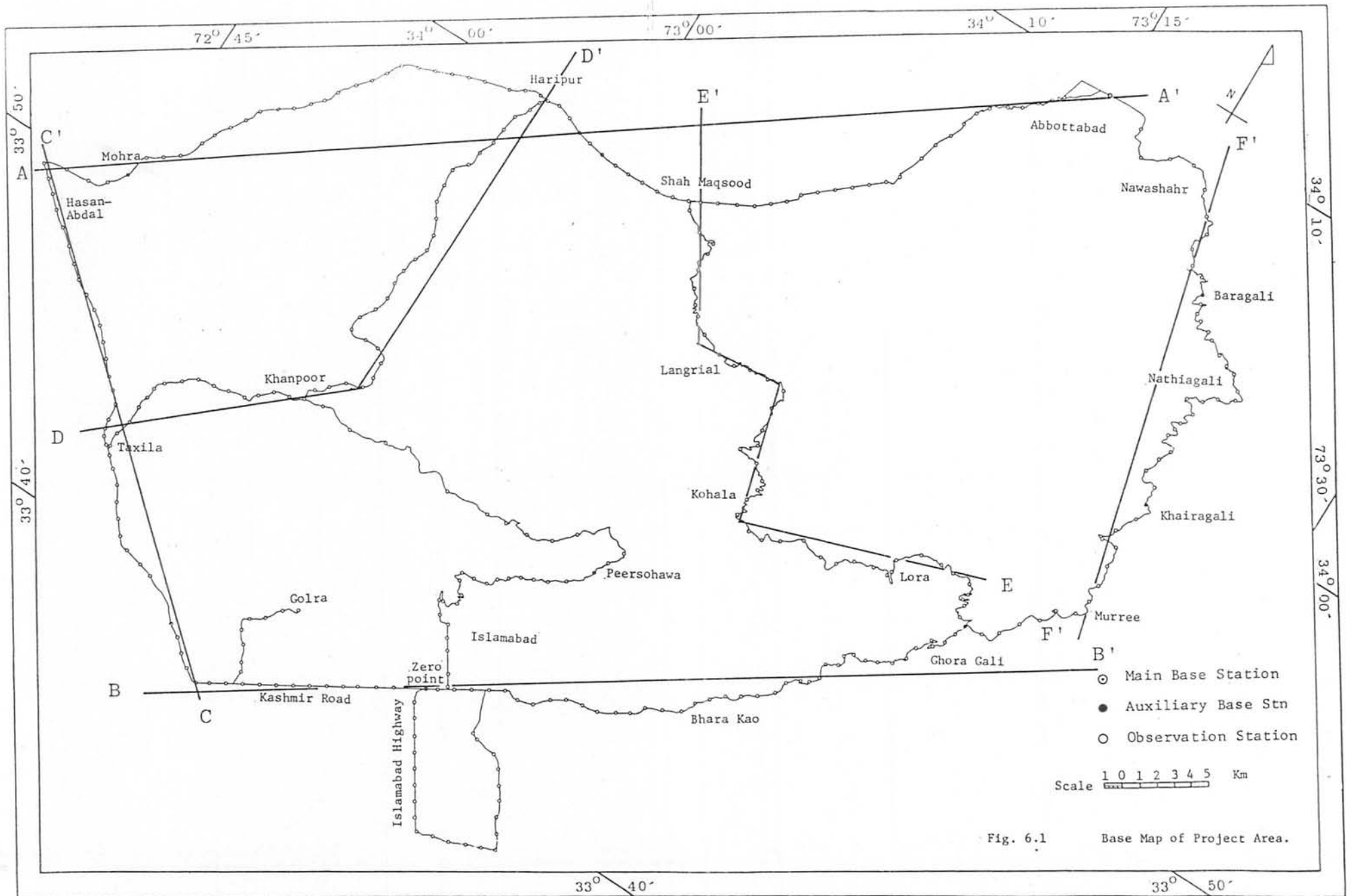
Trend Surface method was tested on observed field data sequentially from first degree to higher degrees. But the results obtained from second degree trend surface are more promising due to the following reasons;

- i) Goodness of fit is more than 80%.
- ii) Regional and residual pictures compare reasonably with those obtained graphically.
- iii) The estimated regional trends are same as expected.



INTERPRETATION

CHAPTER-6



## 6.1 INTERPRETATION:

### 6.1.1 General:

From world-wide gravity measurements, it has been found that the average Bouguer anomaly on land, at the sea level, is approximately zero, in oceanic areas it is generally positive, while in the continental regions it is mainly negative. These variations in gravity are caused by subsurface density changes, and indicate that the material beneath the oceans is denser than the normal, while in elevated land-masses it is lighter.

The Bouguer anomaly calculated in the surveyed area ranges from -213 mgal to -172 mgals. These values agree with those mentioned by Seeber and Armbruster (1979), and suggest that the rocks of low density form a thick sedimentary column in the area.

## 6.2 QUALITATIVE INTERPRETATION:

Gravity interpretation is based on an integrated study of gravity and magnetic maps prepared from the collected data and the available geological maps of the area.

Since the surveyed roads form the curved or wavy sections in the area, the collected data along these roads, thus, have been projected, after processing, on straight lines for the purpose of interpretation. These sections, therefore, exaggerate the actual geographical trends of the road profiles. The details of the exaggerated profiles are given on the next page.

<u>Profile</u>	<u>Route</u>	<u>Direction</u>
A-A'	Hasanabdal to Abbottabad	SW-NE
B-B'	Rawalpindi to Murree	SW-NE
C-C'	Rawalpindi to Hasanabdal	SE-NW
D-D'	Taxila to Haripur	SWW-NEE & SSW-NNE
E-E'	Ghoragali to Shah Maqsood	SEE-NWW & SE-NW
F-F'	Murree to Abbottabad	SSE NNW

The processed gravity data used for this integrated study include the following maps.

- 1) Elevation Profile Map.
- 2) Free-air Anomaly Profile Map.
- 3) Bouguer Anomaly Profile Map (with and without terrain correction)
- 4) Regional Gravity Anomaly Map.

#### 6.2.1 Integrated Study of Elevation and Free-air Anomaly Profiles.

To evaluate the effect of topography on gravity, the free-air anomaly profiles were prepared.

A close examination of Figs. 6.3(a), 6.4(a), 6.5, 6.6, 6.7(a), 6.8(a) suggests that, in general, the elevation trends are correlated with the free-air anomaly picture. Because the free-air reduction is directly related to elevation of the station and is added in the observed gravity (if station lies over mean sea level and vice versa). A dissimilarity between Free-air anomaly and the elevation may be caused by the effect of surrounding terrain or the



subsurface density variations that are not reflected duly, (Figs. 6.3(b), 6.5, 6.6, 6.7(b), 6.8(b)).

It is to be observed along the profile C-C' (Fig. 6.5) that the Free-air anomaly increases with the decrease in elevation at a distance of 4 km from Hasarabdal, and may be indicative of the presence of denser subsurface rocks.

Observation of the profile A-A' (Fig. 6.3(b)) shows that the Free-air anomaly decreases with linear trend of elevation, within a distance of 3 km after Mohra, and suggests the possibility of a contact zone of low and high density rocks. Further on, the trend of Free-air anomaly follows the topography, in general, with the exception of minor deviations on certain points which may be related to some local anomalous masses.

Similarly, along the profile D-D' (Fig. 6.6), the free-air anomaly shows a positive deviation, with respect to regional trend, from the topography at a few points upto 10 kms distance from Haripur, and could be developed by the existence of relatively high density rocks underneath. A negative deviation in Free-air anomaly about 5 km before Haripur, suggests the effect of low density material or the surrounding terrain.

In case of profiles B-B', E-E', F-F' (Figs.6.4(b), 6.7(b), 6.8(b)) the Free-air anomaly generally conforms with the topography.

### 6.2.2 Integrated Study of Free-air Anomaly And Bouguer Anomaly (Without Terrain Correction) Profiles:-

This comparative study is performed to reveal the effects of the anomalous mass distributions above and below the datum plane. The Bouguer and Free-air anomalies near Margalla Pass, along Grand Trunk Road, between Rawalpindi and Hasanabdal (Profile C-C', Fig. 6.5), are unrelated to Free-air anomaly, and may be due to a thick overburden. Whereas near Hasanabdal, the Bouguer anomaly shows much higher values than the free-air anomaly, describing the presence of denser limestones (Eocene to late Jurassic).

It is to be noted that along Hazara Trunk Road, between Hasanabdal to Shah Maqsood Profile A-A' (Figs. 6.3(a), 6.3(b)) both the anomalies follow the same trend and further towards Abbottabad, their behaviour becomes opposite, and may be due to mass deficit beneath the elevated region due to a sudden rise in elevation.

Similarly, the study of Profile B-B' (Figs. 6.4(a), 6.4(b)) which is parallel to the strike, like that of Profile A-A' (Figs. 6.3(a), 6.3(b)), shows that between Rawalpindi and Chattar, both the profiles have similar trend, but from Chattar onwards, the Bouguer anomaly with some exception is continuously decreasing possibly due to higher density used for Bouguer correction to bring data on the sea level. In Profile E-E' which represents the route Ghoragali to Shah Maqsood (Fig. 6.7(a), 6.7(b)), the trends of the free-air and the Bouguer anomalies change from Phalla to an extent of 3 km because of the smoothing effect of Bouguer correction calculated with the selected density of the rock types occurring in the area. About 3 km after Langrial towards Shah Maqsood, the free-air anomaly shows up and down against the static behaviour of

Bouguer anomaly. The free-air anomaly again decreases 5 km before Shah Maqsood, and may be representing the presence of thick alluvium cover.

From Taxila to Haripur (Profile D-D': Fig. 6.6), both the curves follow the same trend, with the exception of an elevated segment of 10 km between Taxila and Khanpur where they behave oppositely. A rapid decrease in free-air and Bouguer anomalies observed at about 9 kms from Haripur strongly suggests a fault contact. Onwards upto Haripur, a thick column of alluvium can be envisaged.

#### 6.2.3 Integrated Study Of Bouguer Anomaly Profiles With And Without Terrain Correction:-

The comparative study of all these profiles (Figs. 6.3(a), 6.4(a), 6.5, 6.6, 6.7(a), 6.8(a)), reveals that the terrain correction has made the anomalies more sharper and prominent. But around Langrial the Bouguer Anomaly uncorrected for Terrain (Fig. 6.7(a)) have been washed out.

The effects of Terrain Correction are more prominent between Murree and Abbottabad (Fig. 6.8(a)). Some new anomalies of small magnitude have appeared. Terrain Correction has suppressed two major gravity lows; one near Khairagali and the other near Nawashahr.

#### 6.2.4 Interpretation Of Bouguer Anomaly Profiles in Context of Geological And Tectonic Maps:-

The Grand Trunk Road, between Rawalpindi and Hasanabdal, obliquely crosses the geological structures related to the Main Boundary Thrust Zone. As the density

contrast between the post-collisional and pre-collisional formations is very low, the Bouguer Anomaly profile shows slight variations along this route. On the left end (Coca Cola Factory) of the traverse C-C' (Fig. 6.5), the gravity behaviour over the exposed sandstone (dipping towards north west) is a positive peak and slowly decreases onwards where it is covered by an alluvium layer. Near Margalla Pass where the Eocene limestone suddenly outcrops, the Bouguer anomaly fluctuates accordingly. About 2 km before Margalla Pass, a rapid decrease in Bouguer anomaly confirms underthrusting of Murrees beneath the limestones (Eocene and Older). This could be a boundary of MBTZ. After 3 km from Margalla Pass, the limestone is buried and gravity value starts falling again upto a point 7 km to reach Hasanabdal. This corresponds to the thickening of alluvium cover and/or the north western dip of the Main Boundary Thrust. Near Wah Cantt and onwards, the much higher gravity values over the exposed limestone may be the indication of shallow presence of Cretaceous limestones under the Eocene limestone.

The Profile E-E', from Ghoragali to Shah Maqsood (Fig. 6.7(a)), crosses major geological structures and the rock units, Eocene limestones to Precambrian Hazara slates. About 4 km after Ghoragali and upto Phalla, the Bouguer gravity generally shows a smooth character over Eocene limestone, however, two small gr. lows in that segment mark the contacts of overlying Lei Conglomerates. Near Kohala, sharp changes in gravity anomaly are generated at the contact of Eocene to Paleocene formations, and similarly the effect of Cretaceous to Paleocene rock units is also described by gravity upto Langrial. From Langrial to Shah Maqsood, high gradient in Bouguer anomaly infers the presence of a fault between Precambrian Hazara Slates and limestones (Eocene and Older) as shown in Fig. 2.2.

filled with low density material comprising of bands of clay and conglomerates of Havelian group (Latif, 1970). After Ghoragali, the Bouguer anomaly shows positive tendency over the outcropping Eocene limestones.

#### 6.2.5 Qualitative Interpretation Of Regional Gravity Anomaly Map:-

Regional gravity anomaly map reveals that the sub-surface structures presented by second degree Trend Surface are opposite to those of surficial geology, i.e., the regional structures dip towards northeast as compared to northwestern dips observed in the field. Since the Precambrian slates in the northeast of the area are involved in thrusting process, the regional trend can be attributed to crystalline rocks lying beneath the Precambrian Hazara slates.

According to Seeber and Armbruster (1979), the occurrence of a decollement zone, beneath Hazara, at a depth of 12-20 kms based on earthquake data and unpronounced seismicity above this depth strongly suggests that there is a layer of plastic material below the sedimentary and metamorphic stratum which damps out the effect of stresses expected to reach the surface. If we assume that there exists a layer of salts between crystalline basement and overlying material, then it could be stated that during collision process of Indo-Pakistan shield with the Eurasian blocks of Afghanistan, Turan and Tarin, stresses were compensated by uplifting and deformation of sediments including metamorphic layer, and crystalline unit did not participate actively in complex deformational pattern due to the presence of intervening salt layer.

The profile F-F', along Murree to Abbottabad road (Fig. 6.8(a)), also runs across the geological structures. It is to be observed that within a distance of 2 km from Murree, there is a sudden rise in Bouguer anomaly corresponding to the change in lithology from Miocene Murrees to limestones (Eocene to Older). From Khairagali to Kuzagali, the Bouguer anomaly shows similar character as that is observed in profile E-E'. From Kuzagali to Nathiagali, a sudden decrease of 15 mgals in Bouguer anomaly reflects that a fault developed within the limestones of Eocene to late Jurassic. Between Nathiagali to Baragali, a positive change in the Bouguer anomaly shows that Eocene limestones is underthrusting the Precambrian Hazara Slates as shown in Fig. 2.2.

The Profile A-A', (Fig. 6.3(a)) which runs along the regional structures of the area, covers a section between Hasanabdal to Abbottabad. The Bouguer gravity anomaly in this profile gently decreases from Mohra and reaches minimum just 4 km before Haripur, and then starts rising upto Shah Maqsood. This broad gravity low is an indication of a basin like structure in which recent sediments of low density seem to be deposited directly on the Hazara slates as shown in Fig. 2.2. After Shah Maqsood to Abbottabad, the Bouguer anomaly does not reflect any important feature except for minor negative deviations which may be associated with variations in the thickness of overlying young Lei Conglomerates.

The Profile B-B' (Fig. 6.4(a)), between Rawalpindi to Murree, is almost parallel to Profile A-A' i.e. along regional strike, and shows similarity in gravity picture over the Murree formation. A gravity low developed between Zero point and Ghoragali, corresponds to a narrow trough

This suggests that the basement which was originally dipping towards northeast (Seeber and Armbruster, 1981) retained its originality during tectonic deformation happened in Eocene and later, and which is responsible for generating opposite structural trends in the overlying formations as are observed.

### 6.3 QUANTITATIVE INTERPRETATION:

#### 6.3.1 Two-dimensional Modelling:-

The quantitative interpretation needs reasonable density contrast, whereas in our case the density contrast between the basement and the overlying sediments is very low except for a small area where Holocene deposits are directly lying on the Precambrian basement (Hazara Slates). The profile A-A' (Fig. 6.3(a), 6.3(b)) which represents the later situation qualifies the basic condition of modelling and is selected for interpretation. Two-dimensional computer modelling based on Talwani's method (1959) is shown in Fig. 6.9.

It is to be examined that with the use of densities 2.0 gm/cc and 2.5 gm/cc for Holocene deposits and the slates respectively, the calculated gravity curve for the segment Hasanabdal to Shah Maqsood gives an excellent fit with the observed Residual Gravity curve. It should also be noted that the same density contrast (0.53 gm/cc) is assumed between Holocene sediments and limestones (Eocene to late Jurassic) on the left flank. The limestone outcropping at Hasanabdal is inferred to be underlying the basement (Hazara slates) near Mohra. The model also shows that the maximum thickness of the sediments is roughly 400 metres at 5 km before Haripur (station 8). The gradient of the

anomaly suggests a low angle thrust fault in the southwestern part of the area between limestone and Hazara slates.

### 6.3.2 Crustal Thickness:-

Crustal thickness calculated from Bouguer anomaly data using different relationships, as discussed in Section 4.7, shows that thickness of the crust is 46 km in the southwest (near Rawalpindi) and increases towards northeast upto 49.0 km near Khairagali. From these thicknesses it appears that Moho is dipping at  $1^{\circ}$  towards north and  $2^{\circ}$  in the northeast direction. These results indicate that the area is isostatically in equilibrium.



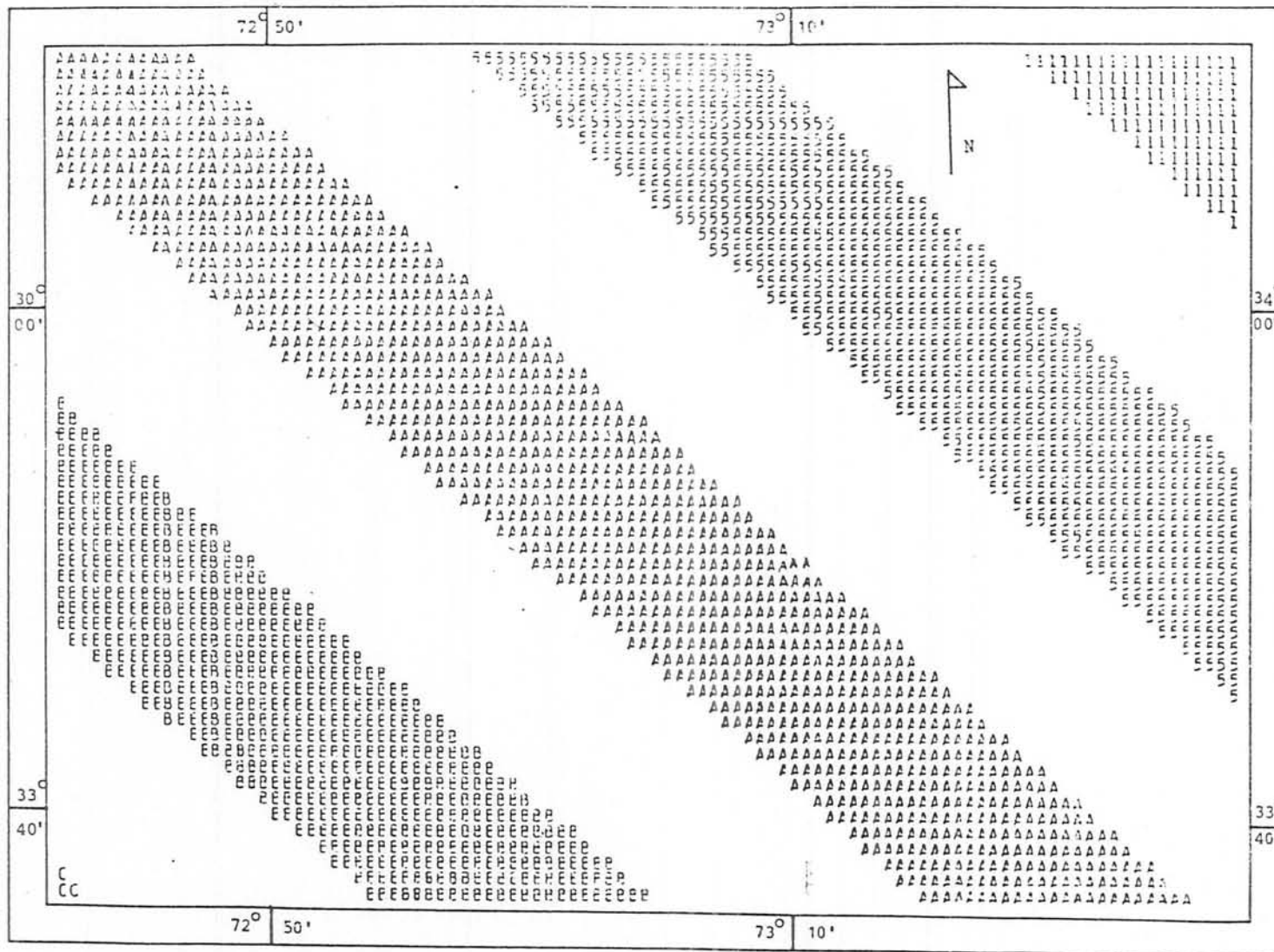


Fig. 6.2: Line printed Regional Bouguer gravity anomaly map. Reference Contour is of  $-200.0$  mgals and represented by '5'. Contour interval is 5 mgals. Values decrease in the north-east direction.

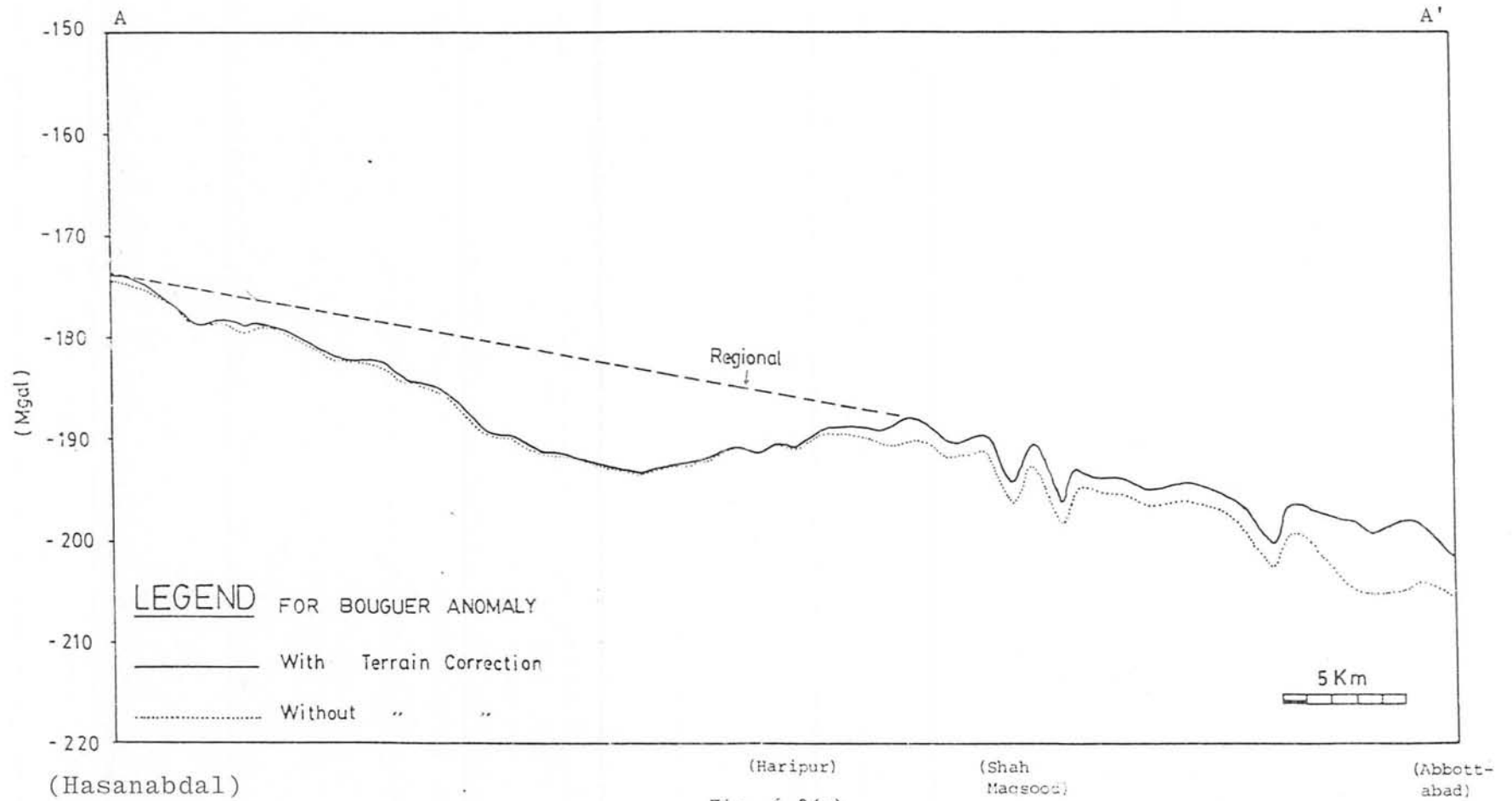
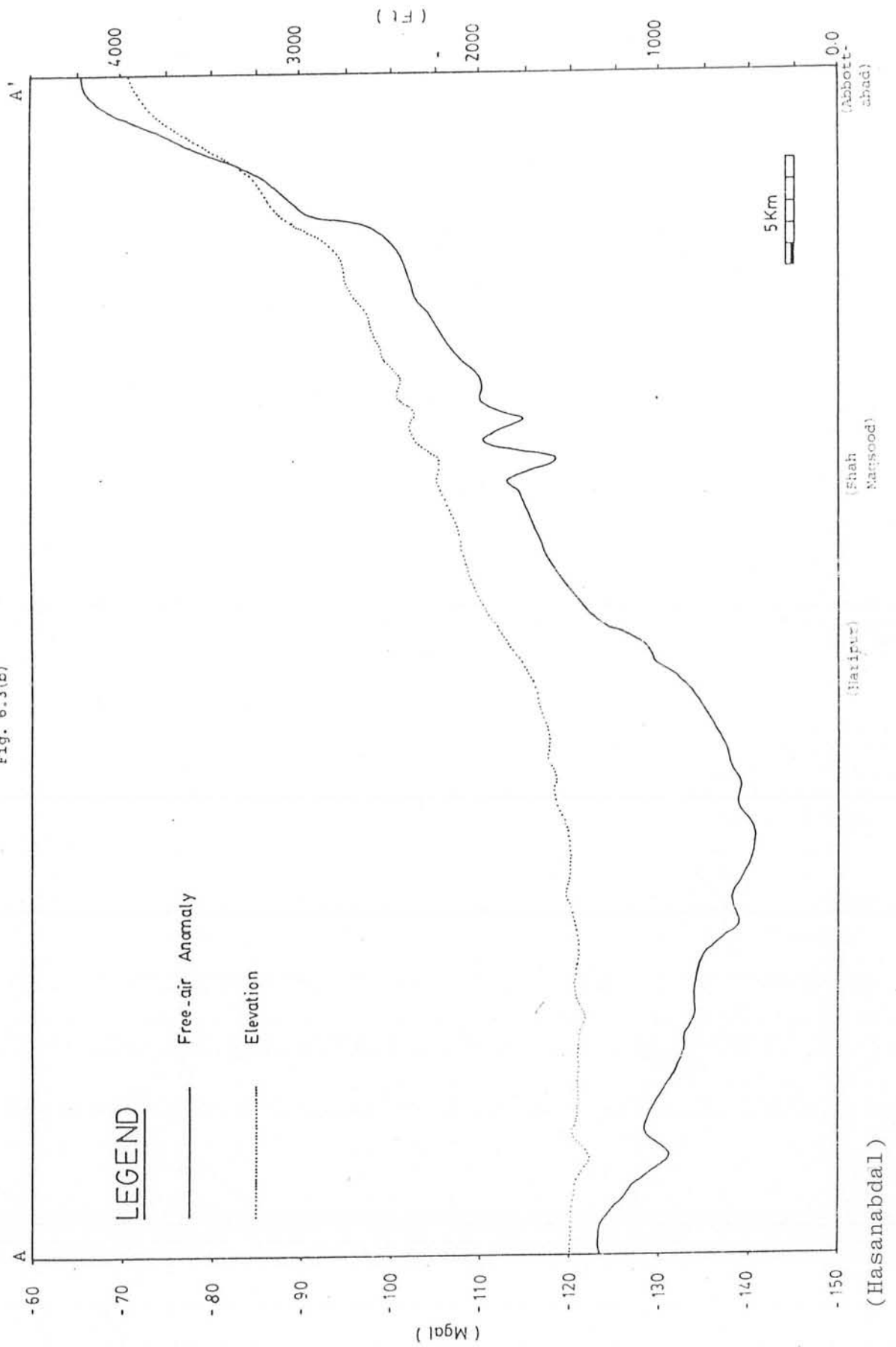


Fig. 6.3(a)

Fig. 6.3(b)



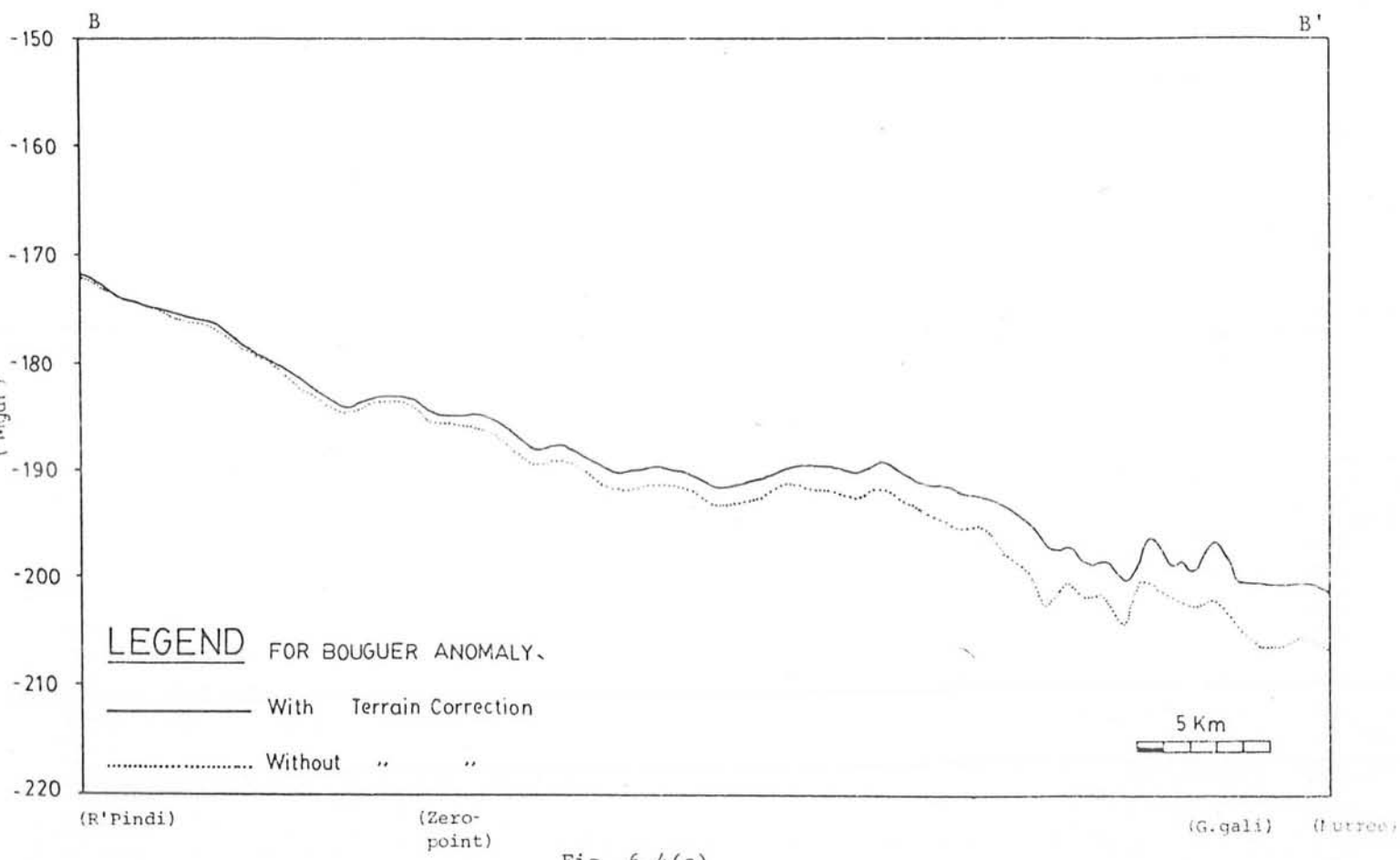
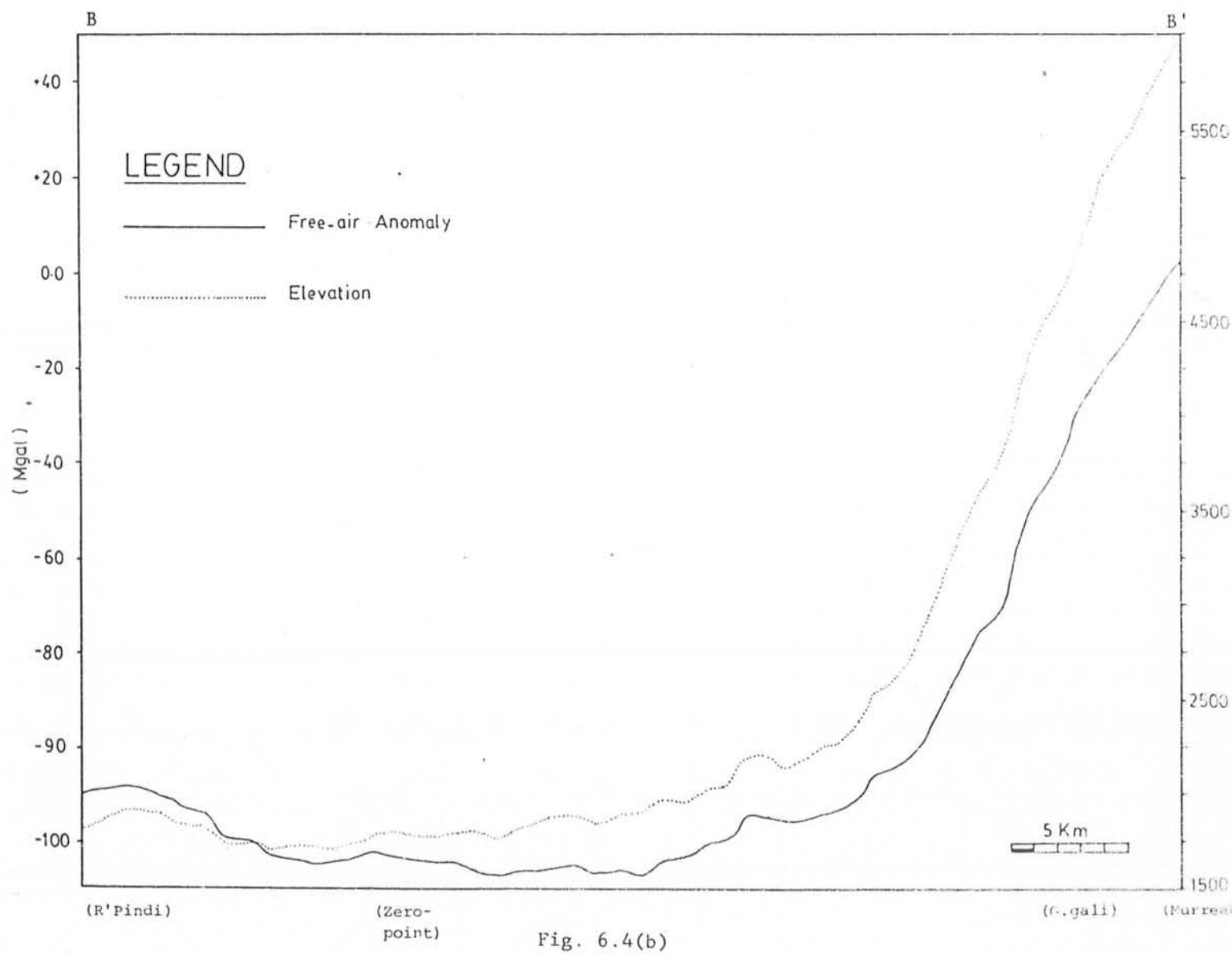


Fig. 6.4(a)



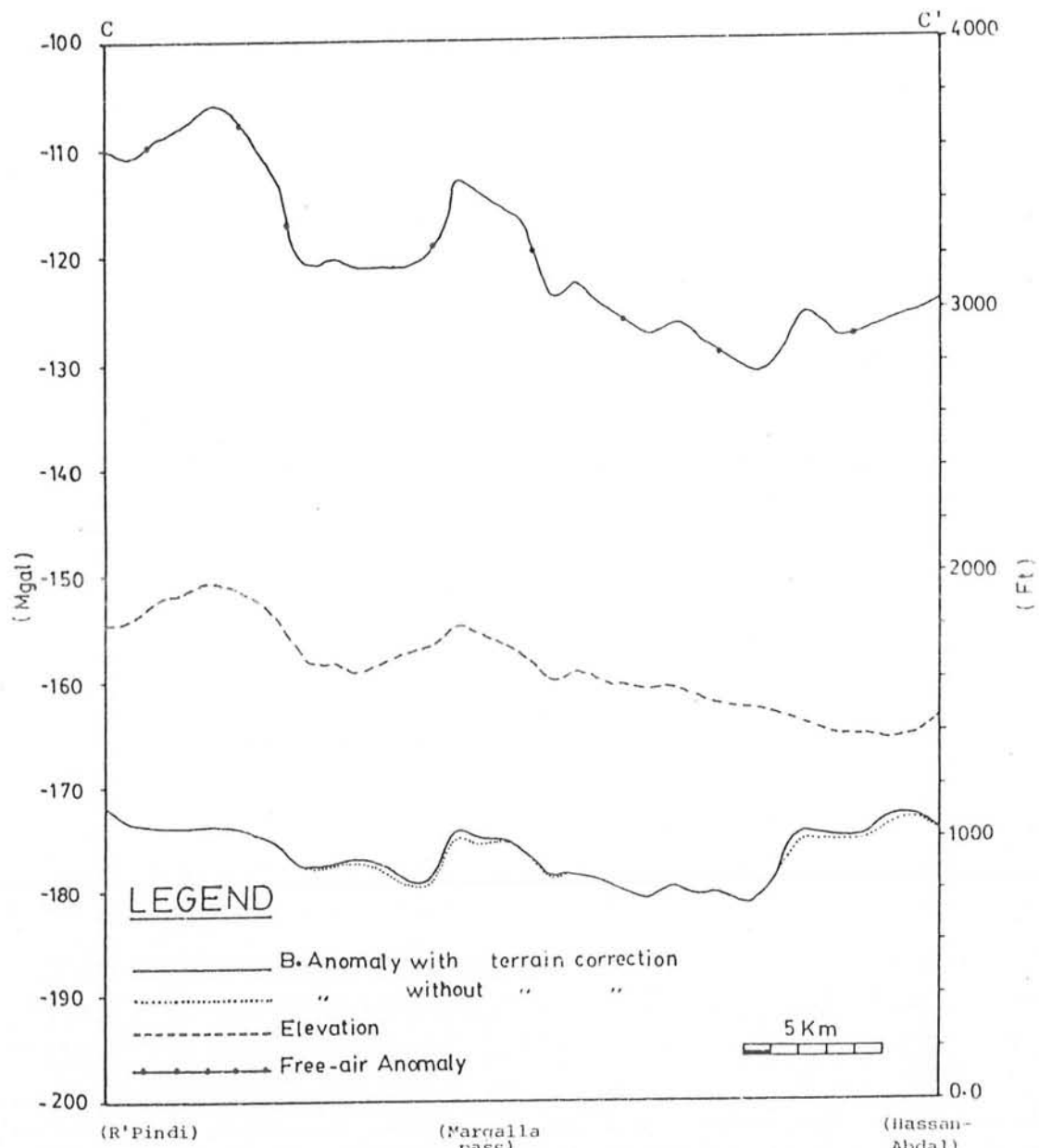


Fig. 6.5

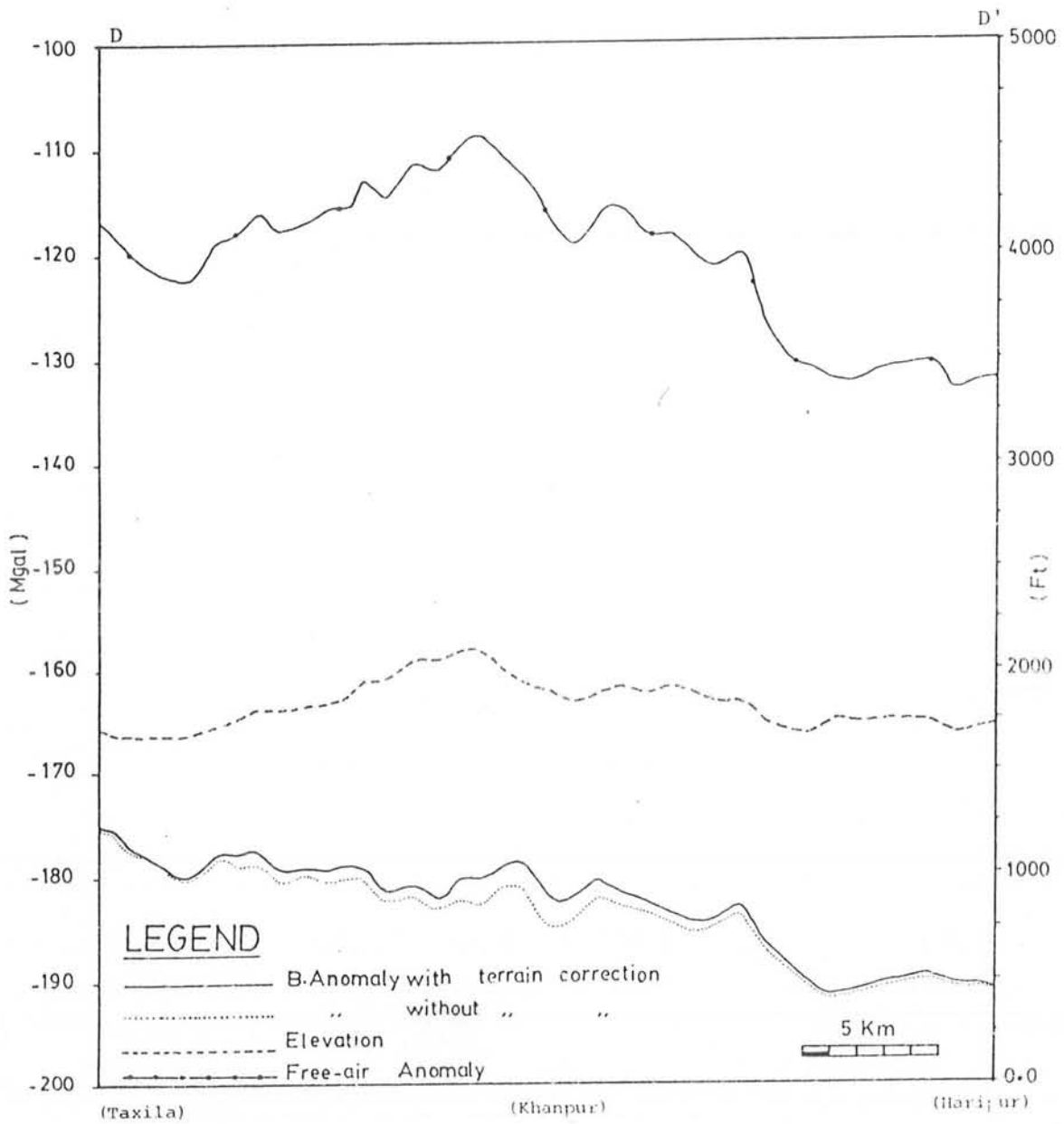


Fig. 6.6

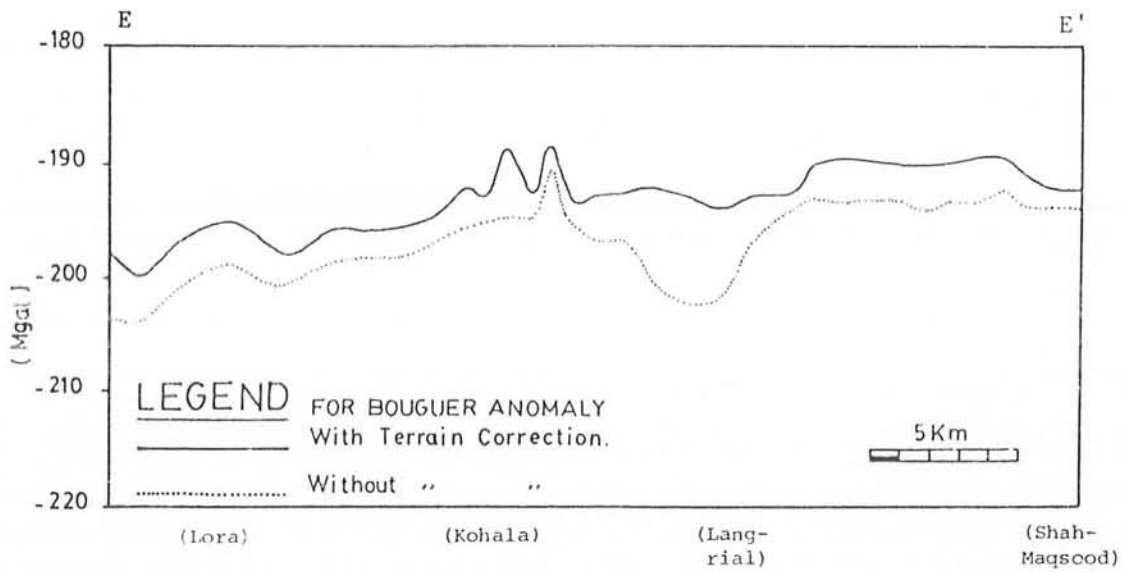


Fig. 6.7(a)



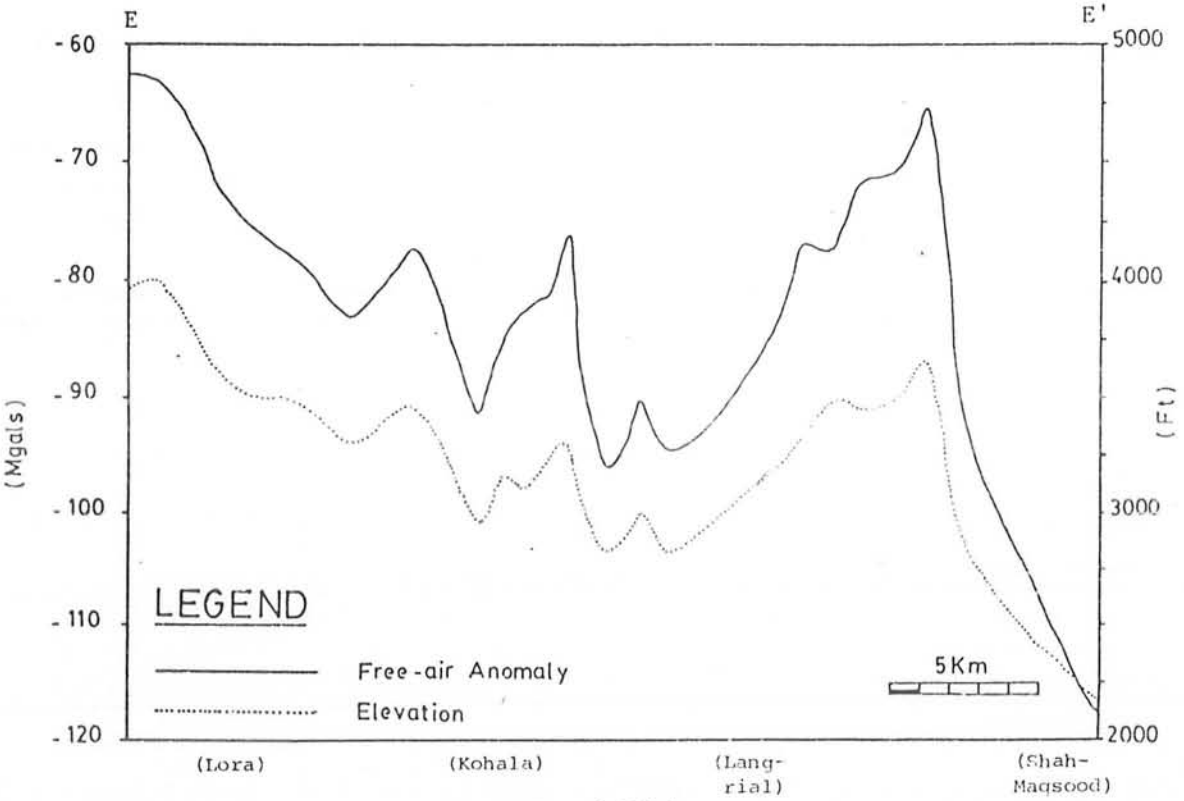


Fig. 6.7(b)

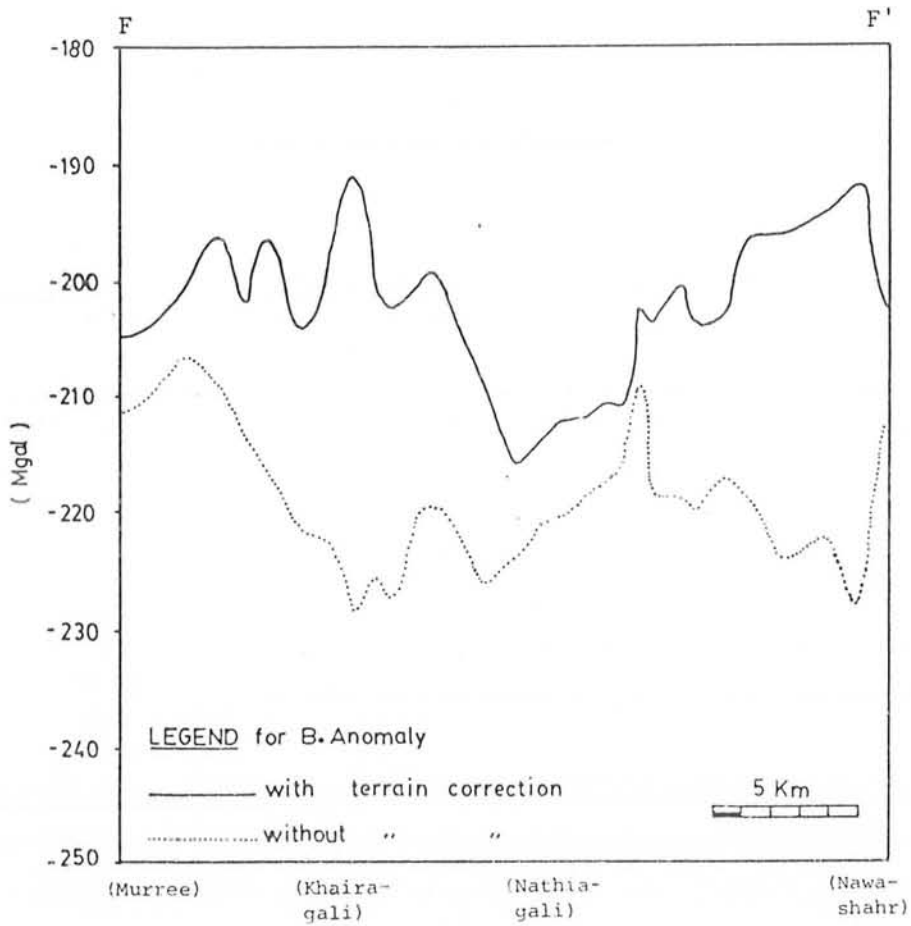


Fig. 6.8(a)

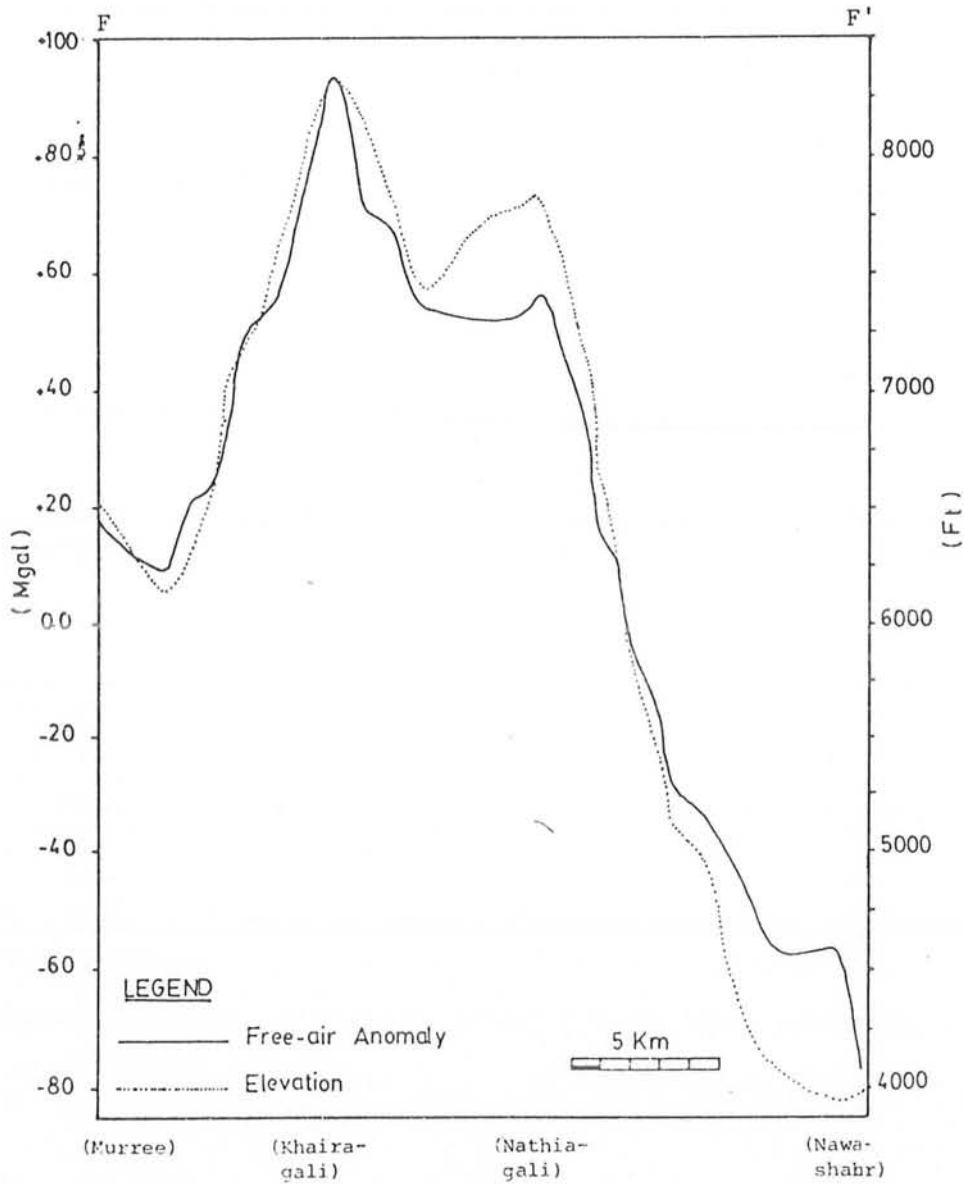


Fig. 6.3(b)

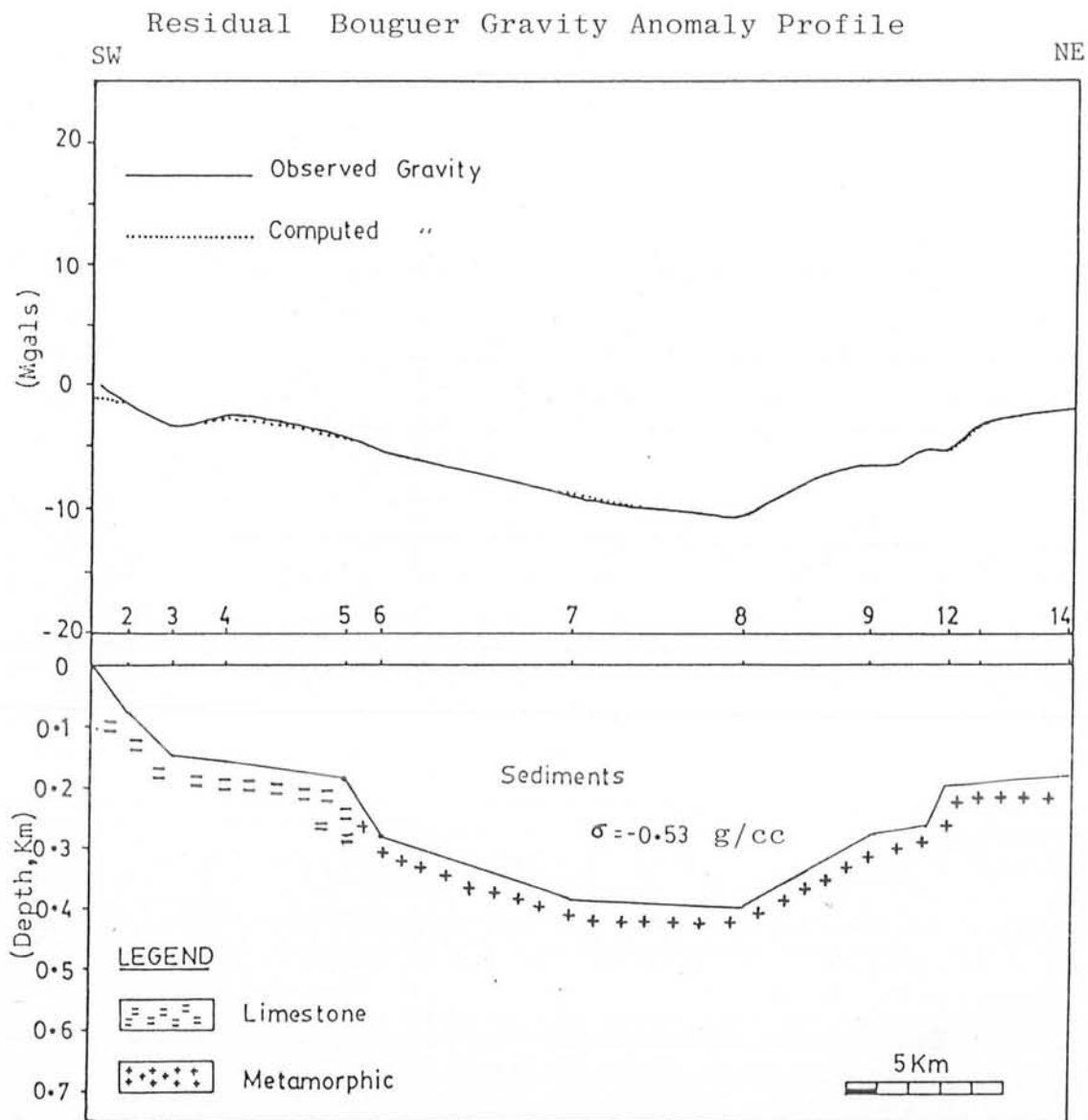
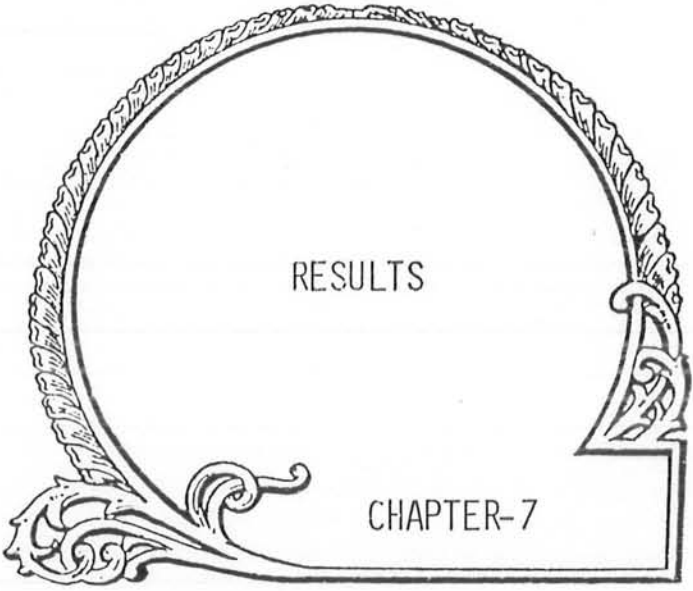


Fig. 6.9: Two dimensional interpretation of part of Profile A-A' (Fig. 6.3(a)). The model shows a basin filled with sediments having maximum thickness of 400 m. The contact between limestones and Hazara Slates Station No. 5-6, is inferred.



RESULTS

CHAPTER-7

## 7.1 DISCUSSION:

The investigated area lies in the western Himalaya region which developed due to continental collision of India and Eurasia about 60 Ma ago. This collision generated many significant features among which are the Hazara Syntaxial belt, the Main Boundary Thrust.

The gravity and magnetic studies on the western limb of the Hazara Syntaxis provide the basis for discussing the surficial and subsurface regional structural patterns. Regional gravity effects attributed to crystalline basement suggest that the basement is dipping in the NE direction as compared to the northwestern dipping exposed lithologies. This is a major contradiction and can be explained if decollement theory of Seeber and Armbruster (1981) is taken into consideration. According to their model when India interacted with Eurasia, a regional system of thrust faults developed all along the orogenic belt. The model for the formation of syntaxis begins with two contrasting portions of the continental shelf of India, one with a thick section of sediments underlain by salt (Hazara region), the second with less sediment and no major effect of salt in the tectonics. The thrusting in the basement as well as in the overlying column remain together where there is no intervening salt layer exists. But where salt layer is present, the coupling between the basement and the overlying sediments is totally disturbed. In this situation effect of stresses on the basement and the surficial materials can not be expected evenly distributed. In other words, the basement behaviour would be different. It looks quite probable in this area that during the northward drifting process of the Indian plate, the overlying sediments did not move with the basement because of the

presence of salt layer and were slipped back easily due to anti-forces generated while pushing the Turan and Tarim blocks. Thus the structures formed in the overlying sediments are different from those of the basement. The salt layer, acting as a damping device, is responsible for reducing the transmission of tectonic forces from overlying column towards basement and vice versa. So we can say that the original basement configuration, that is, NW-SE trend, was not very much disturbed during deformations as happened in the overlying sediments. The regional gravity gradients in the NE corresponds to the original character of the crystalline basement, i.e., dipping towards NE. The overlying structures differing from those of the basement, are then associated with the residual gravity anomalies.

The surficial geological structures dipping in the NW-SE direction, bear a system of thrust faults associated to the limb of Hazara Syntaxis. Residual gravity picks MBT and defines its northeast extension to be observed near Margalla Pass (Taxila), Ghoragali and Kuldana (Murree). An offshoot of MBT being masked by low density sediments, between Hasanabdal and Haripur, is inferred to be lying near Mohra, Khanpur and evidently marked near Langrial and Nathiagali. This offshoot is resulted due to thrusting of Precambrian Hazara Slates over the limestones (Eocene to late Jurassic). The two-dimensional modelling attempted in this area could be done successfully only in the basinal regions because of the reason that sufficient density contrast as required in modelling technique could be attained in these zones. In other areas as appreciable density contrast does not exist between sandstone and limestone, the modelling was abandoned.

## 7.2 CONCLUSIONS:

The conclusions of gravity and magnetic studies around Margalla and Hazara ranges are summarized as follows:

- (I) The north easterly decrease in the Bouguer anomaly (from -172 mgals in Rawalpindi to -213 near Nathiagali) suggests a thickening of low density sediments to that direction.
- (II) The traverses along the regional strike reveal the presence of two narrow troughs on the north-western and southeastern boundary of the area along Hazara Trunk Road and Kashmir Road, Islamabad respectively. The inter-relationship of these basins is not understood clearly because of insufficient data, however, it seems that the trough on the southern boundary is older than that on the northern boundary.
- (III) The Hasanabdal Haripur basin modelled with a density contrast 0.53 g/cc gives 400 m as the maximum thickness of recent sediments.
- (IV) The lack of appreciable density contrast between post-collisional and pre-collisional sediments did not allow modelling of the traverses across the strike of the area.
- (V) The gravity profiles across the geological structures describe the north-eastern continuation of the MBTZ boundary from Margalla Pass to Ghoragali and Murree.



- (VI) Similarly, an offshoot of MBTZ picked near Mohra seems to be continued to Khanpur (Profile D-D', Fig. 6.6), Langrial (Profile E-E', Fig. 6.7(a), 6.7(b)) and Nathiagali (Profile F-F', Fig. 6.8(a), 6.8(b)).
- (VII) The gravity behaviour along G.T. Road, between Margalla Pass and Wah Cement Factory, shows a localized small basin, with maximum thickness of sediments to be 100 m lying over Eocene limestone.
- (VIII) The northwest-southeast trend of regional gravity contradicts the generalized surface geological structures and seems to be associated to the crystalline basement deepening in the NE direction.
- (IX) The calculated crustal thickness in the area also increases towards north-east from 46 km (near Rawalpindi) to 49 km near Khairagali.
- (X) The crystalline basement shows a dip of 1 degree in the north and increases to 2 degrees towards north-east direction.

REFERENCES

## REFERENCES:

1. Bott, M.H.P. 1958, The Use of Electronic Digital Computers For The Evaluation Of Gravimetric Terrain Corrections, Exploration Geophysics. 1958, P. 45.
2. Choudhury & Datta 1975, Crustal Thickness In North India And Himalayan Region And Its Geological Significance, Geophysical Research Bulletin, Vol. 13, Nos. 1 & 2.
3. De Sitter, L.U. "STRUCTURAL GEOLOGY", McGraw Hill, Inc. 1964.
4. Dobrin, Milton . B. "Introduction To Geophysical Prospecting" McGraw Hill Inc., 1981.
5. Gupta, H.K. & F.M.Delany . 1981, "Zagros. Hindukush. Himalaya Geodynamic Evolution" Geodynamics Series, Vol. 3.
6. Gansser, A., The Significance Of The Himalayan Suture Zone, Tectonophysics, 62 (1980) 37-52.
7. Iqbal, M.W.A. & S. M.I. Shah. "A Guide To The Stratigraphy Of Pakistan", Geological Survey Of Pakistan, 1980.
8. Jain, A.K., Goel, R.K. & N.J.K. Nair. Implication of Pre-mesozoic Orogeny in the Geological Evolution of the Himalaya and Indo-Gangetic Plains. Tectonophysics 62: 67-86.
9. Narain, H. 1980, Overview of Some Recent Geophysical Investigations in Himalaya, Tectonophysics, 62:

10. Nettleton, L.L. "Geophysical Prospecting For Oil", McGraw Hill, Inc., 1940.
11. Parasnis, D.S. "Principles of Applied Geophysics" Chapman & Hall, London, 1972.
12. Powell, C. McA., A Speculative Tectonic History Of Pakistan and Surroundings: Some Constraints From the Indian Ocean, In: Geodynamics Of Pakistan, (eds.) A. Farah and K. A. DeJong, Geol. Surv. Pakistan, Quetta, 5-24, 1979.
13. Qureshi, I.R. & H.G. Mula 1971, Two-dimensional Mass Distributions From Gravity Anomalies: A Computer Method, Geophysical Prospecting. 19, 180-191.
14. Tahir Kheli, R.A.K., Mattauer, M., Proust, F., and P. Tapponier . The India Eurasia Suture Zone In Northern Pakistan: Synthesis and Interpretation Of Recent Data at Plate Scale, In: Geodynamics of Pakistan, (eds.) A. Farah, and K.A. DeJong, Geol. Surv. Pakistan, Quetta, 125-130, 1979.
15. Telford, W.M. & Others; "Applied Geophysics", Cambridge University, London, 1976.

A P P E N D I C E S

## APPENDIX-A

AUTOMATIC DETERMINATION OF SURFACE DENSITY BY NETTELETON METHOD.

DIMENSION T(50,50),G(50),E(50),DC(50),H(50),DEN(10),SLOPE(50),GD(50),FA(50

#),BA(50,50),GM(50),BF(50),X(50)

DATA SLOPE,GRC,N,M,FF,BF/50\*0,0.0902,14,8,0.3086,0.04185/

GRC=CALIBRATION CONSTANT,M=NO OF DENSITIES USED FOR BOUG.CORR,N=NO OF POIN

NO STATION IN A PROFILE.

READ (\*,10) (DEN(I),I=1,M)

10 FORMAT (8F5.2)

READ (\*,20) (T(I),G(I),E(I),X(I),I=1,N)

DF=((G(N)-G(1))/(T(N)-T(1)))\*GRC

DO 30 J=1,M

DO 40 I=1,N

BF(J)=BF\*DEN(J)

GM(I)=G(I)\*GRC

H(I)=E(I)-E(1)

DC(I)=(T(I)-T(1))\*DF

FA(I)=FF\*H(I)-DC(I)

BA(I)=FA(I)-BF(J)\*H(I)

40 WRITE(\*,50) GM(I),H(I),DC(I),FA(I),BA(I),J)

30 WRITE(\*,60) DEN(J),BF(J)

50 FORMAT (/2X,'FOR DENSITY=',F10.3,4X,'B.C.FACTOR=',F10.5)

60 FORMAT (/2X,5F10.6)

STIN=X(2)-X(1)

DO 70 J=1,M

SLOPE(J)=(BA(2,J)-BA(1,J))/STIN

INDEX=1

DO 80 J=1,M

IF(SLOPE(INDEX).GT.S(J)) INDEX=J

80 CONTINUE

SMIN=SLOPE(INDEX)

DENF=DEN(INDEX)

WRITE(\*,90) SMIN,DENF

90 FORMAT (/2X,'MINIMUM SLOPE=',F10.6,'FINAL DENSITY=',F10.3)

STOP

END

## APPENDIX-B

```

5 REM: GRAVITY DATA PROCESSING IN GW.BASIC; SYSTEMS: -IBM-PC, XT & TANDY (1000-1200)
6 DIM B1(100), E(100), L1(100), T(100), L2(100), F1(100), B1(100), G2(100), S(100)
7 DIM COT(100)
8 REM: G1=OBSERVED GRAVITY, G2=CORR. GRAVITY DIFFERENCE, E=ELEVATION OF OBS. STNS
9 REM: TO DEFINE FUNCTION TO CONVERT TIME INTO MINUTES.
10 REM: TO READ CONSTANT PARAMETERS AND DEFINE NEW CONSTANTS.
11 READ C1, C, B, G0, D, N
12 B0=G0*B : C0=C*60 : C2=.612776*D
13 REM: C1=CALIBRATION CONST. OF GRAVIMETER, B0, D ARE LATITUDE CORR. FACTORS.
14 REM: GRAVITY AT THE EQUATOR, D=DENSITY USED FOR BOUGUER CORR.
15 REM: C4=ABS. GRAVITY VALUE AT THE BASE S.N. N=NO OF LOOPS.
16 REM: TO READ INPUT DATA AND PERFORM COMPUTATIONS.
17 FOR J=1 TO N
18 READ C4, M, NAMEL#
19 FOR I=1 TO M
20 READ S(I), T(I), E(I), G1(I), L1(I)
21 COT(I)=INT(T(I))*60+(T(I)-INT(T(I)))*100
22 NEXT I
23 DR=(G1(M)-G1(1))/(COT(M)-COT(1))
24 PRINT SPC(5) "LOOP NO="; J; "FROM" SPC(1) NAMEL#
25 PRINT SPC(5) "GRAVITY AT THE BASE="; C4; "Mgals"
26 PRINT SPC(5) "DRIFT RATE="; DR; "S.D/MIN"
27 FOR I=1 TO M
28 G2(I)=C1*(G1(I)-G1(M)-DR*(COT(M)-COT(I)))+C4
29 L2(I)=G0+B0*((SIN(L1(I)))^2)-C0*(SIN(L1(I)*2))^2
30 FAC=FCF*E(I)
31 BC=C2*E(I)
32 EC=FAC-BC
33 F1(I)=G2(I)-L2(I)+FAC
34 B1(I)=F1(I)-BC
35 IF (I=1) THEN GOSUB 350 ELSE 310
36 PRINT USING "###"; S(I);
37 PRINT USING " #####.##"; E(I), G1(I), L2(I), EC, F1(I), B1(I)
38 PRINT "-----"
39 NEXT I
40 NEXT J
41 GOTO 390
420 PRINT "*****"
430 PRINT "STN" SPC(3) "ELEVATION" SPC(2) "OB-GRAVITY" SPC(2) "Th-GRAVITY" SPC(3) "ELEV-
CORR" SPC(2) "FA-ANOMALY" SPC(2) "BG-ANOMALY"
440 PRINT "*****"
450 RETURN
460 REM: DATA FOR CONSTANTS AND INPUT.
470 DATA 0.0902, 0.0000359, 0.0052384, 978047, 2.67, 1
480 DATA 979344.5, 4, "R'PINDI TO MURREE"
490 DATA 1, 10.25, 1800, 1350, 35.2
500 DATA 2, 10.4, 1805, 1349, 35.4
510 DATA 3, 10.5, 1820, 1345, 35.6
520 DATA 1, 11, 1800, 1349.5, 35.2
530 END

```

# APPENDIX-C

```

C      PROGRAM TO SEPARATE REGIONAL AND RESIDUAL EFFECTS FROM OBSERVED DATA.
C      THIS PROGRAM IS BASED ON W-PLATE RING METHOD OF LAYTON, 1961, P. 117.
C
C      STN=STATION NUMBER, AM=FIELD ANOMALY, RGM=REGIONAL EFFECT, RSM=RESIDUAL
C      N=NO OF ROWS, M=NO OF COLUMNS, R=RADIUS OF THE CIRCLE.
C
C      DIMENSION STN(40,26),AM(40,26),RGM(40,26),RSM(40,26)
C      READ(1,10) N,M,R
C      WRITE (3,10) N,M,R
C      DO 999 I=1,M
C      DO 999 J=1,N
C      AM(I,J)=0.0
C      RGM(I,J)=0.0
C      RSM(I,J)=0.0
999  CCNTINUE
C      READ(1,20)((STN(I,J),AM(I,J),J=1,N),I=1,M)
2)  FCORMAT(8(A4,F6.0))
C      DO 111 I=1,M
101  WRITE(3,111)(STN(I,J),AM(I,J),J=1,N)
111  FCORMAT(7(2X,A4,2X,F10.2))
C      CCNTINUE
C      S=R*SQRT(2.0)
C      K1=N-1
C      K2=M-1
C      TC CHECK A POINT WITH DATA AND PROCESS AND STORE THE RESULT.
C      DO 30 I=2,K2
C      DO 30 J=2,K1
C      A1=AM(I,J)
C      IF(A1.EQ.0.0)GO TO 3)
C      A=0.0
C      B=0.0
C      C=0.0
C      D=0.0
C      E=0.0
C      C1=0.0
C      IF (AM(I-1,J).EQ.0.0) GO TO 4)
C      C1=C1+1.0
4)  IF (AM(I,J+1).EQ.0.0) GO TO 45
C      C1=C1+1.0
45  IF(AM(I+1,J).EQ.0.0) GO TO 5)
C      C1=C1+1.0
5)  IF(AM(I,J-1).EQ.0.0) GO TO 55
C      C1=C1+1.0
55  IF(AM(I-1,J-1).EQ.0.0) GO TO 6)
C      B=A1+((AM(I-1,J-1)-A1)/S)*R
C      C1=C1+1.0
6)  IF(AM(I-1,J+1).EQ.0.0) GO TO 65
C      C=A1+((AM(I-1,J+1)-A1)/S)*R
C      C1=C1+1.0
65  IF(AM(I+1,J+1).EQ.0.0) GO TO 7)
C      C=A1+((AM(I+1,J+1)-A1)/S)*R
C      C1=C1+1.0
7)  IF(AM(I+1,J-1).EQ.0.0) GO TO 75
C      E=A1+((AM(I+1,J-1)-A1)/S)*R
C      C1=C1+1.0
75  IF (C1.EQ.0.0) GO TO 3)
C      A=AM(I-1,J)+AM(I,J+1)+AM(I+1,J)+AM(I,J-1)
C      SUM=A+B+C+D+E
C      RGM(I,J)=SUM/C1
C      RSM(I,J)=A1-RGM(I,J)
3)  CCNTINUE
C      WRITE (3,140)
C      WRITE(3,130)
C      WRITE (3,140)
C      ICCOUNT=)
C      OUTPUT THE RESULTS FOR STATIONS WITH DATA.
C      DO 110 I=1,M
C      DO 110 J=1,N
C      IF (AM(I,J).EQ.0.0) GO TO 11)
C      ICCOUNT=ICCOUNT+1
C      WRITE(3,120) ICCOUNT,STN(I,J),AM(I,J),RGM(I,J),RSM(I,J)
C      WRITE(3,130)
C      IF(MOD(ICCOUNT,4).EQ.0) GO TO 8)
C      GO TO 11)
8)  IF(I.GE.M) GO TO 11)
C      WRITE (3,140)
C      WRITE(3,130)
C      WRITE (3,140)
110  CCNTINUE
C
C      STCP
1)  FCORMAT(2I5,F5.0)
1.1) FCORMAT(1X,'SNO',7X,'STATION',10X,'T-ANOMALY',10X,'REGIONAL',10X,'R',
#RESIDUAL')
12) FCORMAT (14,9X,A4,10X,F10.2,8X,F10.2,8X,F10.2)
13) FCORMAT (74(' '))
14) FCORMAT (74(' '))
C      END

```





```

WRITE(3,2006) SSC,NDF2,AMSD
WRITE(3,2007) SST,NDF3
WRITE(3,2008) R2,R
IW=WIDTH*10.0
IF=WIDTH*8.*(X2MAX-X2MIN)/(X1MAX-X1MIN)
CX1=(X1MAX-X1MIN)/FLOAT(IW-1)
CX2=(X2MAX-X2MIN)/FLOAT(IF-1)
WRITE(3,2009)
X2=X2MAX
CC 121 I=1,IF
X1=X1MIN
CC 122 J=1,IW
JB=1
CC 124 K=1,ICRD
CC 125 L=1,K
JB=JB+1
KB=JB-K
C(JB)=C(KB)*X1
125 CCNTINUE
JB=JB+1
C(JB)=C(KB)*X2
124 CCNTINUE
Y=C(J)
CC 126 K=1,ICRD2
Y=Y+B(K)*C(K)
126 CCNTINUE
IY=((Y-REFC)/CIAT)+7.005
IF(IY.LT.1) IY=2
IF(IY.GT.13) IY=2
ICUT(J)=ICHR(IY)
X1=X1+CX1
122 CCNTINUE
WRITE(3,2010) (ICUT(J),J=1,IW)
X2=X2-CX2
121 CCNTINUE
WRITE(3,2012) REFC,CIAT
WRITE(3,2011) ICRD
STOP
1001 FCRMAT(13,7F8.0)
2001 FCRMAT(1H0,4X,'INPUT DATA MATRIX-',1X,'COLUMNS = VARIABLES, ROWS
# 1 = OBSERVATIONS')
2002 FCRMAT(1H0,4X,'COLUMN1 = X1, COLUMN 2 = X2,',1X,
# 'COLUMN 3 = Y, COLUMN 4 = ESTIMATED Y,COLUMN 5 = DEVIATION')
2003 FCRMAT(1H0,4X,'TREND SURFACE COEFFICIENTS',5X,
# '1 = CONSTANT TERM')
2004 FCRMAT(1H)SOURCE OF , 13X,25HSUM OF DEGREES OF FREEDOM,/,
# 10H VARIATION,3X,37HSQUARES FREEDOM SQUARES TEST,/,
# 1X,60(1H-))
2005 FCRMAT(11H REGRESSION,10X,F10.2,18,2X,F10.2,/,9X,F10.4)
2006 FCRMAT(10H DEVIATION,11X,F10.2,18,2X,F10.2)
2007 FCRMAT(16HOTOTAL VARIATION,5X,F10.2,18)
2008 FCRMAT(10GCOEFFICNESS OF FIT = ',F10.4,/,
# 'CORRELATION COEFFICIENT = ',F10.4)
2009 FCRMAT(1H1)
2010 FCRMAT(1X,100A1)
2011 FCRMAT(1H0,4X,'TREND SURFACE MAP OF DEGREE ',12)
2012 FCRMAT(1H0,4X,'REFERENCE CONTCUR = ',F10.4,5X,'CONTOUR INTERVAL = '
# ,F10.4)
END
SUBROUTINE READM(A,N,M,N1,M1)
DIMENSION A(N1,M1)
C READ SIZE OF THE MATRIX
READ(1,1000) N,M
C READ MATRIX ONE ROW AT A TIME
CC 100 I=1,N
READ(1,1001) (A(I,J),J=1,M)
100 CCNTINUE
RETURN
1000 FCRMAT(2I3)
1001 FCRMAT(5X,2F10.4,24X,F8.2)
FAC

```

```

SUBROUTINE PRINTM(A,N,P,N1,M1)
DIMENSION A(N1,M1)
PRINT MATRIX OUT IN STRIPS OF P COLUMNS
C 1-10 IB=1,M,10
IE=IB+9
IF(IE-M) 2,2,1
1 IE=M
C 2 PRINT HEADING
WRITE(3,2000) (I,I=IB,IE)
C 101 CC 101 J=1,N
PRINT ROW OF MATRIX
WRITE(3,2001) J,(A(J,K),K=IB,IE)
101 CCNTINUE
100 CCNTINUE
RETURN
2000 FCRMAT(1H1,1X,10I12)
2001 FCRMAT(1F0,15,10F12.4)
ENC
SUBROUTINE SLE(A,B,N,N1,ZERC)
DIMENSION A(N1,N1),B(N1)
CC 100 I=1,N
DIV=A(I,I)
IF (ABS(DIV-ZERC))99,99,1
1 CC 101 J=1,N
A(I,J)=A(I,J)/DIV
101 CCNTINUE
B(I)=B(I)/DIV
CC 1-2 J=1,N
IF(I-J) 2,102,2
2 RATIO=A(J,I)
CC 1-3 K=1,N
A(J,K)=A(J,K)-RATIO*A(I,K)
103 CCNTINUE
B(J)=B(J)-RATIO*B(I)
102 CCNTINUE
100 CCNTINUE
RETURN
99 CALL EXIT
ENC

```



```

2 FCORMAT(6I5)
3 FCORMAT(3F5.2,2F10.5,4F3.1)
WRITE (3,4) GRID,DENSTY,SCALE1,SCALE2,SCALE3,SD1,SD2,SD3,SD4

C
C      CALCULATION OF CONSTANTS.
SC1=SC1**2
SC2=SC2**2
SC3=SC3**2
SC4=SC4**2
FGRID=0.5*GRID
FGRISQ=FGRID**2
GRICSC=GRID**2
FGRISC=4.0*GRICSC
C2=.012776*DENSTY
C3=C.005*DENSTY
CCNST=(6.673*DENSTY*GRIDSQ*(SCALE2**2))/(2.001*SCALE3)

C
9 WRITE (3,9) NUMST,NBLCK,CCNST
FCORMAT (1J,1T20,NUMBER OF STATIONS=1,10,/,T20,
A 'NUMBER OF BLOCKS='18,/,T20,'CONSTANT ='1,15.9,/,
4 FCORMAT ('0',1T20,'GRID='1,10.0,/,T20,'DENSITY='1,10.0,/,T20,
C 'SCALE 1='1,10.0,/,T20,'SCALE 2='1,11.5,/,T20,'SCALE 3='1,11.5,/,
C //,T20,'SD 1='1,10.0,/,T20,'SD 2='1,11.0,/,T20,'SD 3='1,11.0,/,
C T20,'SD 4='1,10.0,/)
IF (IACPNT.NE.2) GO TO 13
WRITE (3,11)
11 FCORMAT (11,'BLCK NO. '1X,'XXXX',4X,'YYYY',4X,'1111 '1,'2222 '1,
A '3333 '1,'4444 '1,'5555 '1,'6666 '1,'7777 '1,'8888 '1,'9999 '1,
B '1010 '1,'1111 '1,'1212 '1,'1313 '1,'1414 '1,'1515 '1,'1616',/)

C
12 FCORMAT(2X,13,2F10.2,3X,16(2X,14))
13 CCNTINUE

C
C      STATION DATA PREPARATION.
CC 20 I=1,NUMST
REAC(10,22) NOST(1),XST(1),YST(1),HST(1),FAA(1),CORSC(1)

C
HST(1)=FSTN(1)*SCALE1
FHSTSQ(1)=4.0*(HST(1)**2)
FHSTSC(1)=4.0*FHSTSQ(1)
ABGPRV(1)=FAA(1)-C2*(HST(1)-ELBASE)-1.09416*ELBASE
CCRNSC(1)=C3*CORS(1)
CCR(1)=0.0
NREJ1(1)=0
NREJ2(1)=0
NREJ3(1)=0
NREJ4(1)=0
NCBLCK(1)=0
21 CCNTINUE
22 FCORMAT(15,2F8.4,F8.2,16X,F8.2,5X,F8.4)

C
C      BLOCK DATA PREPARATION.
CC 50 M=1,NBLCK

C
REAC(11,24) IXBLCK,IYBLCK,IH
XBLCK=FLCAT(IXBLCK)
YBLCK=FLCAT(IYBLCK)
IF (IACPNT.NE.2) GO TO 23
WRITE (3,12) M,XBLCK,YBLCK,IH
IF (MCC(M,5).EQ.0) WRITE (3,79)
IF (MCC(M,40).EQ.0) WRITE (3,11)
23 CCNTINUE
24 FCORMAT(18I4)

C
CC 26 I=1,16
F(I)=FLCAT(IH(I))
CCNTINUE

C
ICTH=0.
ICTSCH=0.

C
CC 30 I=1,4
CALL CCCRC(I,XBLCK,YBLCK,GRID)
XSUB(I)=XXXX
YSUB(I)=YYYY
SUMF=0.
SUMSCH(I)=0.

C
CC 29 J=1,4

CALL CCCRC(J,XSUB(I),YSUB(I),GRID)
X(I,J)=XXXX
Y(I,J)=YYYY
FFF=F(K(I)+L(J))
SUMF=SUMF+FFF
SUMSQH(I)=SUMSQH(I)+FFF**2
FF(I,J)=FFH

C
29 CCNTINUE

SUMTH(I)=SUMF**2
ICTH=ICTH+SUMTH(I)
ICTSCH=ICTSCH+SUMSQH(I)
30 CCNTINUE

C
C      TESTING OF DISTANCE BETWEEN STATION AND BLOCK POSITIONS.
CC 40 I=1,NUMST
RSC=(XBLCK-XST(I))**2+(YBLCK-YST(I))**2
IF(RSC.GT.SD1) GO TO 40
NCBLCK(I)=NCBLCK(I)+1
IF(RSC.GT.SD2) GO TO 35

C
CC 39 II=1,4
RSC=(XSUB(II)-XST(I))**2+(YSUB(II)-YST(I))**2
IF(RSC.GT.SD3) GO TO 36
CC 38 JJ=1,4
RSC=(X(II,JJ)-XST(I))**2+(Y(II,JJ)-YST(I))**2
IF(RSC.GE.SD4) GO TO 37

```

```

C
CC      REGISTRATION OF REJECTED SQUARES.
NREJ=K(II)+L(JJ)
IF(NREJ1(I).EQ.0) GO TO 31
IF(NREJ2(I).EQ.0) GO TO 32
IF(NREJ3(I).EQ.0) GO TO 33
NREJ4(I)=NREJ
GC TO 38
31 NREJ1(I)=NREJ
GC TO 38
32 NREJ2(I)=NREJ
GC TO 38
33 NREJ3(I)=NREJ
GC TO 38

C
C      CALCULATION AND ADDITION OF TERRAIN CORRECTION.
37 HSC=(HST(I)-FH(II,JJ))*2
R=SQRT(RSQ)
TERC=HSC/(R*(RSQ-FGRISQ))
CCR(I)=CCR(I)+TERC
38 CCNTINUE
GC TO 39

C
36 HSC=HSTSQ(I)+SUMSQH(II)-HST(I)*SUMTH(II)
R=SQRT(RSQ)
TERC=HSC/(R*(RSQ-GRIDSQ))
CCR(I)=CCR(I)+TERC
39 CCNTINUE
GC TO 40

C
35 HSC=SHSTSQ(I)+TCTSQH-TCTH*HST(I)
R=SQRT(RSQ)
TERC=HSC/(R*(RSQ-FGRISQ))
CCR(I)=CCR(I)+TERC
40 CCNTINUE

C
50 CCNTINUE

C
C      PRINT OUT.
C      PRINT OUT.
C      PRINT OUT.
56 WRITE (3,56)
FCRMT ('1',T10,'TERR.CORRECTED POUQUER G. ANGLY FOR STATIONS IN
A.....,/)
57 WRITE (3,57)
FCRMT ('1',ST.NO. PREV.ANGM. TR.CCR. PRG.ANGM. TR.CCR. BU.ANGM.
ANBLK ST.NO. TER.CCR. ( R E J E C T I O N ) X-CCCR. Y-CCCR.
PHEIGHT',/,
C (MCL.) PRG. PRG.CORCT REJ.SCS. (NBL)
C
C      TOTAL',/)

C
CC 74 I=1,NUMST
CCR(I)=CCR(I)*CCNST
ABGTPC(I)=ABGPRV(I)+CCR(I)

C
IF (ICCRSQ.NE.2) GO TO 58
CCRTOT(I)=CCRNSC(I)+CCR(I)
111 ABGFJA(I)=ABGPRV(I)+CCRTOT(I)
WRITE (3,75) NOST(I),ABGPRV(I),CCR(I),ABGTPC(I),CCRNSC(I),
A ABGFJA(I),NCBLCK(I),NCST(I),CCRTOT(I),NREJ1(I),NREJ2(I),NREJ3(I),
B NREJ4(I),XST(I),YST(I),HST(I)

C
C      SAVING OUTPUT.
IF (ISAVE.NE.2) GO TO 59
WRITE (12,81) NCST(I),XST(I),YST(I),HST(I),ABGPRV(I),CCRTOT(I),
C ABGFJA(I)
GC TO 59

C
58 WRITE (3,76) NOST(I),ABGPRV(I),CCR(I),ABGTPC(I),NOST(I),
A NREJ1(I),NREJ2(I),NREJ3(I),NREJ4(I),XST(I),YST(I),HST(I)

C
59 IF (MCC(I,5).EQ.0) WRITE (3,79)
IF (MCC(I,40).EQ.0) GO TO 68
GC TO 74
68 IF (I.GE.NUMST) GO TO 74
WRITE (3,56)
WRITE (3,57)
74 CCNTINUE

C
75 FCRMT (15,3X,F7.1,1X,F8.5,4X,F7.1,3X,F6.1,4X,F7.1,2X,F5.2,1X,
A 2X,F6.1,2X,416,2F11.2,F9.2)
76 FCRMT(15,3X,F7.1,3X,F8.5,4X,F7.1,3X,':',4X,':',11X,15,9X,
A 2X,416,2F11.2,F9.2)
79 FCRMT (' ')

C
81 FCRMT (15,2F11.2,4,4F8.2)

C
IF (NXTSET.EQ.2) GO TO 6

C
99 STOP
ENC
SUPERCUITINE COORD (III,)>>>,YYY,CCG)
CCMCMN >>>>,YYY
>>>>>>>+CCG+((-1.)**III)
IF(III.GT.2) GC TO 12
YYY=YYY+CCG
GO TO 12
12 YYY=YYY-CCG
13 RETURN
ENC

```

# APPENDIX-F

000000

```

PROGRAM TO CALCULATE THE THICKNESS OF THE CRUST.
  NUMST=NC OF STATIONS.,BA=BOLGNER ANOMALY,DELTA=STATION CORRECTION
  DIMENSION BA(400),T1(400),T2(400),T3(400),T4(400),RAV(400),AVG(400)
  C),NCST(400)
  NUMST=360
  F=FLUAT(NUMST)
  CC 1J I=1,NUMST
10 REAC (12,11)  MOST(I),BA(I)
  WRITE (3,13)
  CC 15 I=1,NUMST
  T1(I)=33.-0.455*BA(I)
  T2(I)=35.*(1.-TANH(0.0037*BA(I)))
  T3(I)=30.-0.1*BA(I)
  T4(I)=32.-0.18*BA(I)
  RAV(I)=(T2(I)+T3(I))/2.
  AVG(I)=(T1(I)+T3(I)+T4(I))/3.
  WRITE (3,20) I,MOST(I),T1(I),T2(I),T3(I),T4(I),RAV(I),AVG(I)
15 CONTINUE
  STCP
11 FCRMAT (15,44X,F3.2)
13 FCRMAT (8X,'S-NC',5X,'ST--NO',8X,'THICK-1',8X,'THICK-2',8X,'THICK-3',
  C',8X,'THICK-4',8X,'RUSAVG',9X,'TAVG'//)
20 FCRMAT (/5X,15,5X,15,6(5X,F10.2))
  END
  
```

:

## APPENDIX-G

```

10 REM:PROGRAM FOR TWO-DIMENSIONAL GRAVITY MODELLING BY TALWANI'S METHOD(1959).
15 REM:THIS PROGRAM IS IN GW.BASIC & CAN BE RUN ON IBM-PC,IBM-XT,TANDY(1000-1200
)
20 REM:THIS PROGRAM NEEDS INPUT OF CO-ORDINATES AND OBSERVED GRAVITY.
30 REM:OUTPUT IS GIVEN AT THE END OF EACH CYCLE FOR SELECTED ADJUSTMENT.
40 REM:PROGRAM DEVELOPED BY MOHAMMAD.ARSHAD,EARTH SCIENCES DEPTT.Q.A.Univ,ISD.
50 DIM G1(50),G2(50),X(50,50),X1(50),Z(50),TT(50),STN(50)
60 DIM Z2(50),T(50),T2(50),R2(50),X2(50,50),R1(50),Z1(50)
70 INPUT "PROFILE=";P#
80 READ N,G,D,Z0,D1,ADJUSTMENT1,S
90 REM:N=NO OF POINTS,G=GRAVITATIONAL CONSTANT,D=DENSITY CONTRAST.
100 REM:Z0=DEPTH TO SURFACE OF ANOMALOUS BODY.
110 REM:D1=MIN.DIFF. OF OBSERVED AND COMPUTED GRAVITY TO BE APPROACHED.
120 REM:S=SCALE CONSTANT.
130 LPRINT
140 LPRINT
150 LPRINT
160 M=N-1 : C3=2*G*D
170 C0=3.14*C3 : N3=N-2
180 INPUT "ADJUSTMENT =";ADJUSTMENT
190 IF ADJUSTMENT1=ADJUSTMENT THEN GOTO 200 ELSE 250
200 LET L=10 : C5=C0
210 GOTO 260
220 REM:L=NO OF CYCLES TO BE PERFORMED.
230 REM:STN=STATION NUMBER,X1=CO-ORDINATES OF POINTS .
240 REM:G1=OBSERVED GRAVITY.
250 LET L=6 : C5=.5*C0
260 FOR J=1 TO N
270 READ STN(J),X1(J),G1(J)
280 NEXT J
290 FOR I=1 TO N
300 X1(I)=S*X1(I)
310 Z(I)=Z0+G1(I)/C0
320 Z2(I)=Z(I)^2
330 NEXT I
340 Z1=Z0^2
350 LPRINT SPC(4) "PROFILE=";P#
360 LPRINT "NO OF STN=";N;"G=";G;"DENSITY CONTRAST=";D;"MIN DIFF=";D1
370 FOR I=1 TO N
380 FOR J=1 TO N
390 X(I,J)=X1(J)-X1(I)
400 X2(I,J)=X(I,J)^2
410 NEXT J
420 NEXT I
430 REM:- TO FIND THE LINE INTEGRAL OVER THE TOP & VERTICAL SIDES.
440 FOR I=1 TO N
450 T(I)=Z0*(ATN(X(I,1)/Z(1))-ATN(X(I,N)/Z(N)))
460 TT(I)=.5*(X(I,1)*(LOG((X2(I,1)+Z1)/(X2(I,1)+Z2(1))))+X(I,N)*(LOG((X2(I,N)+Z2
(N))/(X2(I,N)+Z1))))
470 NEXT I
480 LET K=1 : N1=1
490 LET S1=0
500 FOR I=N1 TO N
510 FOR J=1 TO N
520 T2(J)=ATN(X(I,J)/Z(J))
530 R2(J)=X2(I,J)+Z2(J)
540 NEXT J

```





DEDICATED TO  
MY  
PARENTS, BROTHERS AND  
SISTERS